12-2015

Battery Energy Storage System: A Financial Analysis for Microgrids

Nikitas Zagoras
Clemson University

BATTERY ENERGY STORAGE SYSTEM:
A FINANCIAL ANALYSIS FOR MICROGRIDS

A Thesis
Presented to
the Graduate School of
Clemson University

In Partial Fulfillment
of the Requirements for the Degree
Master of Science
Electrical Engineering

---

by
Nikitas Zagoras
December 2015

Accepted by:
Dr. Elham Makram, Committee Chair
Dr. Randy Collins
Dr. Nikolaos Rigas

ABSTRACT

Renewable Energy Sources are becoming more popular mostly due to their reduced carbon footprint. One major issue that keeps them from becoming more popular is their output variability. Energy Storage Systems have been gaining a lot of “traction” into the power grid since they can address that variability and make RES more controllable. In this thesis, various Energy Storage Systems are introduced, while Battery Energy Storage Systems and their various technologies are studied in more detail. BESS are commonly used in supporting Photovoltaic Power Plants, as they provide the convenience of a shared DC bus. This thesis also includes an overview in solar energy technologies in order to assess the complexities of solar energy harvesting, through a PPP.

A mathematical approach that quantifies the financial and operational impacts of a BESS is developed. Specifically, two test cases are investigated: intermittency mitigation of a PPP using a BESS and optimal scheduling of microgrid with BESS. The former problem is formulated as a Mixed Integer Linear Programming problem while the latter is formulated as a Linear Programming problem. Both algorithms provide accurate solutions while achieving optimality. The study concludes with a financial model for the optimal operation of an advanced lead-acid BESS and the outcome is analyzed.

DEDICATION

I dedicate this thesis to the memory of my late father.

ACKNOWLEDGMENTS

I wish to express my gratitude to my advisor, Dr. Elham Makram for her guidance, support, kindness, and patience throughout the period of research and study at Clemson University.

I thank Dr. Randy Collins and Dr. Nikolaos Rigas for their patience and acceptance to be my committee members.

I thank all the fellow students in my research group, especially Karthikeyan Balasubramaniam and Parimal Saraf, with whom I had many fruitful discussions throughout the course of my period at the university.

I thank the Department of Electrical and Computer Engineering and the professors with whom I worked through the course of my masters. They helped me develop and improve my knowledge of electrical engineering.

Last but not the least I want to thank my wife, mother, and sisters who have always been encouraging.

TABLE OF CONTENTS

Table of Contents (Continued)

Page

Table of Contents (Continued)

Page

LIST OF TABLES

LIST OF FIGURES

List of Figures (Continued)

Page

CHAPTER ONE

INTRODUCTION

Thesis Statement

Energy storage systems have been supporting the power grid for many decades. Though the medium that stores the energy might be different, the final goal is always the same; to assist the operator in managing the power system the most efficient way possible while staying within the operating limits. In this study, an energy storage system that relies on the use of batteries, more specifically Advanced Lead-Acid batteries, is investigated. The analysis involves the role of this system into a microgrid that incorporates a Photovoltaic Power Plant. The main hypothesis of this study is that a Battery Energy Storage System (BESS) can add value to a power system and that this value can be quantified. For this reason two optimal scheduling schemes are used, initially the Integer Linear Programming and later the Mixed Integer Linear Programming. The hypothesis is tested when the revenue generated by the BESS is compared to the cost of the system (capital and operational).

Motivation

The motivation behind this study lies on the need to create a more efficient, reliable, environmental friendly and more economical power grid. In order to improve the power grid's effectiveness and efficiency the integration of new tools and solutions is needed. These solution can come from a BESS, as some reports like [1] - [4] have suggested. These

systems have been evolving for decades now and some of them have reached a good maturity level where they have a reasonable cost and great performance. Further analysis on maturity levels of different BESS is presented in Chapter 3. The new need for a more responsive and controllable power grid is also dictated by government mandates that require higher levels of power generation through renewable energy sources like wind and solar farms.

Goals / Objectives

One of the main objectives of this study is to develop a methodology that can be implemented on different microgrid systems that have different characteristics, e.g. different generator model or different PPP constraints, and being able to evaluate the impact of the BESS. An impact that can be monetized to some extent but has also some intangible benefits like increasing the usage levels of renewable energy sources thus reducing carbon dioxide emissions produced from fossil fuel generators. Though the topic of the environmental impact of a BESS can be relevant to some extent, it will not be included in this analysis. By adding the benefits and associated revenues introduced by the BESS into the system and by making a direct comparison between those two, the researcher can draw a conclusion on the feasibility of such an investment. This comparison, which in essence is a cost/benefit analysis; a common approach when a decision making process is needed. The conclusion and the final goal of this study, is to give a the prospective investor an insight of how the system is utilized and how it performs.

Outline of the thesis

The remaining chapters of this thesis are outlined as follows:

Chapter 2: In this chapter, basic concepts of solar energy and different methods of how this energy is harvested are presented. The two major groups of solar energy technologies are introduced, the photovoltaics (PV) and concentrating solar power (CSP). Furthermore, this review introduces PV system components and different structures. Various materials and construction architectures for PV panels and their characteristics are also described.

Chapter 3: In this chapter, a review of the most popular Energy Storage Systems and their typical characteristics is presented. Since the main topic of this thesis is about BESS, once these systems are introduced an in depth analysis of different battery technologies follows. This study will cover Flow batteries, Sodium Sulfur batteries, Lead-Acid and Advanced Lead-Acid batteries, Nickel Cadmium batteries and Lithium-Ion batteries. Finally, a comparative analysis of the different ESS in regards to their maturity level, application based sizing and discharge time concludes this chapter.

Chapter 4: This chapter is the core of this thesis since the methodology used for the BESS financial evaluation is described. The used algorithms (MILP and ILP) are introduced and the problem formulation is defined. Through this process, the equality and inequality constraints of the microgrid system set the problem foundation. Once the foundation is set, the targeted optimal solution is obtained for twelve consecutive calendar years. That is accomplished by using historical data for load demand and solar farm output, which leads to the calculation of the revenues generated by the BESS. A sensitivity analysis

that involves different variable costs and discount rates and how these affect the Net Present Value is then conducted. Finally, a Monte Carlo simulation, which addresses the variability of the revenues generated by the BESS, is introduced.

Chapter 5: In this chapter a conclusion is drawn, which considers all the factors, regarding the feasibility of the BESS addition to the existing microgrid. While the conclusion is based on the analysis made and was mathematically justified, a financial decision is more complicated than that. The reason for that is that many of the factors considered as constant, on the problem formulation, can change. Such examples can be the energy price on different regions or the project financing. A brief discussion about these issues, as well as some ideas about future work conclude this study.

CHAPTER TWO

PHOTOVOLTAIC POWER PLANT

Solar energy: Introduction

Solar energy offers numerous strategic benefits. One such benefit is the reduction of emissions from human-induced greenhouse gases (GHGs) and air pollutants. That happens since solar energy can replace fossil-fuel combustion generators. Moreover, solar technologies have very low operating costs, hence insurance against conventional fuel supply disruptions and price volatility is provided. In addition, growing the solar energy industry could establish and support a growing number of solar-related jobs [3]. In spite of these benefits, solar energy currently supplies only a small fraction of today's energy needs, largely because it historically costs more than conventional energy sources. Nonetheless, solar manufacturing costs and sales prices have dropped dramatically over the past few decades. Experience acquired from past projects has shortened the time and expense required to install a fully operating solar system. These gains originate partly due to research and development (R&D) and partly due to global solar market stimulation. Many experts believe that solar energy is getting mature enough and will be part of the energy solution of the future.

Solar energy: Photovoltaics and Concentrating Solar Power

There are two major categories of solar energy technologies, which are distinguished by the way they convert sunlight into electricity. These categories are the photovoltaics (PV) and concentrating solar power (CSP).

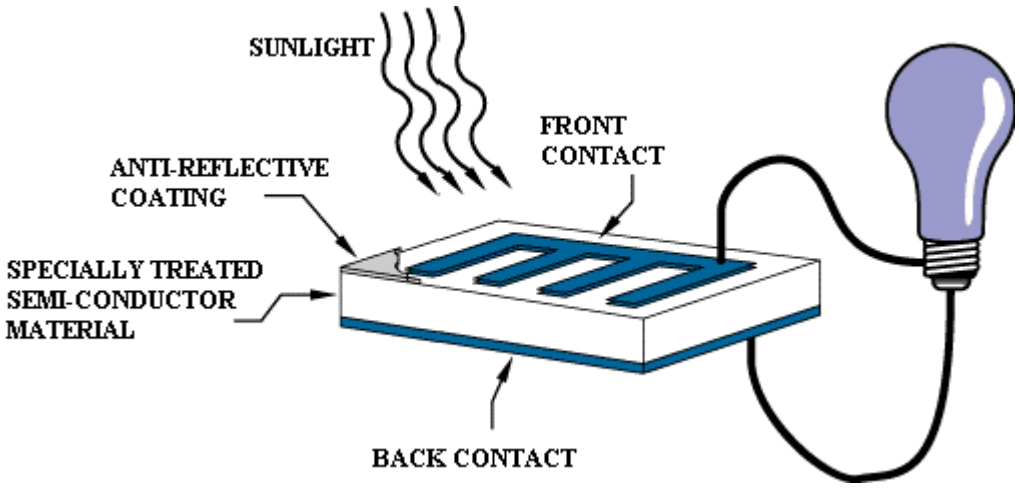

Figure 1: The operation of a basic photovoltaic cell (solar cell) [4]

The PV use a semiconductor material (usually silicon) to convert sunlight directly into electricity. “When sunlight strikes the solar cell, electrons are knocked loose from the atoms in the semiconductor material. If electrical conductors are attached to the positive and negative sides, forming an electrical circuit, the electrons can be captured in the form of Direct-Current (DC) electricity” [4]. For grid-interconnected applications, an inverter transforms DC electricity into alternating current (AC) electricity, which is eventually transmitted and distributed into the power grid. There many different sizes of PV systems,

the variation has to do primarily with the application of the system and consequently with space and budgetary constraints. There are two major categories; the rooftop PV systems and the utility-scale PV. [5]

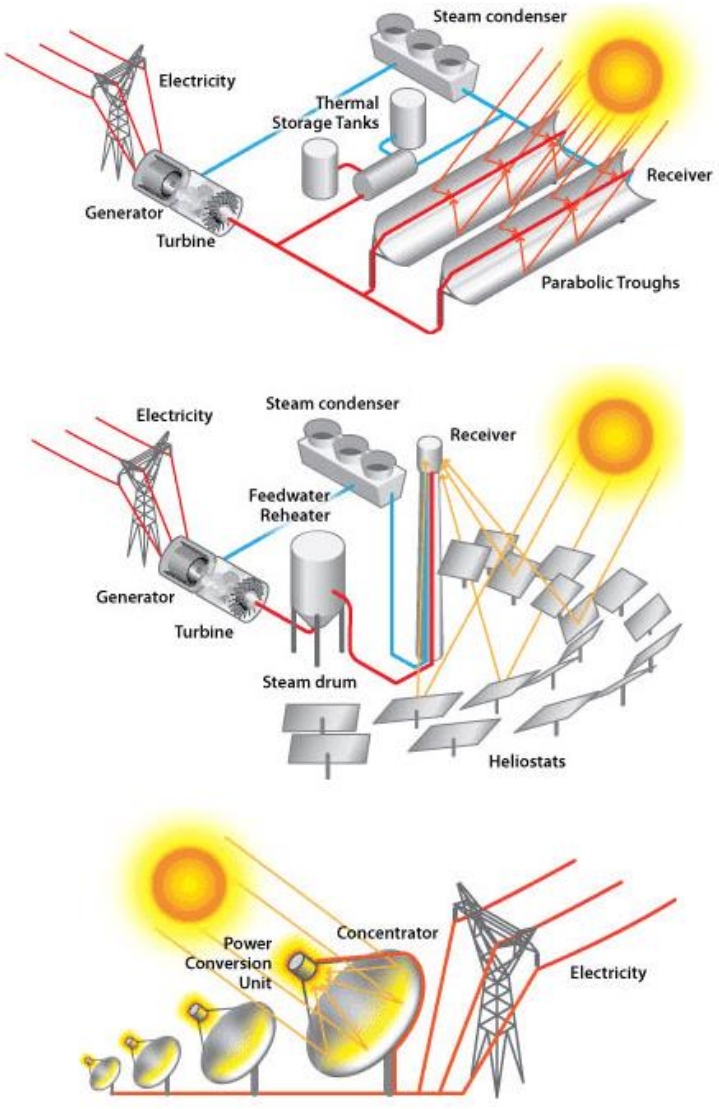

Figure 2: CSP systems: Parabolic Trough (top), Power Tower (middle), Parabolic Dish (bottom) [6]

Small PV systems installed on rooftops and awnings, are called distributed or rooftop PV systems. On a residential level, rooftop PV systems range in size from a few kilowatts (kW) up to hundreds kilowatts, and for large commercial roofs, go up to a few megawatts (MW). Utility-scale PV are usually installed on the ground and range in size from a few megawatts up to hundreds of megawatts. Large utility-scale systems greater than 20 MW are usually interconnected to the power grid at a transmission level which transmits the energy generated from the Photovoltaic Power Plant (PPP) to the electrical substations. Smaller utility-scale systems can be located near areas of higher power demand and be interconnected to the power grid at a distribution level so the energy generated can be distributed from electrical the substations to the consumers.

The CSP systems use mirrors or lenses to concentrate sunlight and produce intense heat, which produces electricity via a thermal energy conversion process similar to those used in conventional power plants. “Several CSP technologies use concentrated sunlight to heat a fluid, boil water with the heated fluid, and channel the resulting steam through a steam turbine to produce electricity. An alternate approach uses gases heated with concentrated sunlight to drive a closed cycle heat engine that produces electricity.” [5]

Although some CSP technologies are capable of being deployed at a distribution level, most are designed for utility-scale operation and are interconnected on a transmission level. CSP systems come in different system configurations, some of these are: Parabolic trough, Linear Fresnel, Power tower, Dish engine [7]. In this study the PV is the system under study hence the analysis of it will take place on the next few sections.

PV system structure and components: Introduction

PV systems can be divided into three subsystems: PV modules, power electronics and Balance-Of-Systems [5]. The PV modules consist of multiple interconnected PV cells that convert sunlight into electric energy. PV cells are constructed from semiconductor materials that allow photons to displace electrons out of their molecular lattice, leaving a freed electron that generates contributes in the generation of DC electricity. This photoelectric effect has been observed with materials such as crystalline silicon (c-Si) and a range of thin-film semiconductors [8]. Since the power grip operates on AC electricity, the DC generated electricity from the PV modules, has to be changed. For that purpose power electronics are used in order to convert and condition AC into DC electricity. The power electronics form inverters that change DC into AC, while a transformer steps the electricity up to the appropriate voltage. Finally, BOS comprises the remaining components required to produce a complete PV system (mounting, wiring, hardware, support structures, power conditioning, land, etc.)

PV system structure and components: PV module technologies

More than a few crystalline silicon and thin-film PV technologies have been used commercially on a large scale but many other types are being researched and tested. Research looks promising and many emerging technologies will increase the competition on a technical and economical level. Below there is a short introduction for the four different PV module categories: crystalline silicon, thin film, concentrating PV and other

emerging technologies. One important PV module attribute is its efficiency and is defined as the percentage of the sun's energy striking the cell or module that is converted into electricity.

a. Crystalline Silicon

   Crystalline silicon (c-Si) technologies constitute about 85% of the current PV market [9]. This technology has a long history of reliable performance; c-Si modules have demonstrated operational lifetime of more than 25 years [10]. There are two different types of c-Si PV, these are: monocrystalline and multicrystalline. "The rated DC efficiencies of standard c-Si PV modules are about 14%–16%. Non-standard cell architectures tend to use high-quality monocrystalline wafers and more sophisticated processing to achieve module efficiencies of about 17%–21%". [5]

b. Thin Film

   Thin films are able to absorb the energy from the sunlight with a much thinner layer than traditional c-Si PV. Thin-film modules have lower DC efficiencies than c-Si modules which ranges in: 9%–12% for CdTe, 6%–9% for a-Si and 8%–14% for CIGS. "The CdTe based PV has experienced significantly higher market growth during the last decade than the other thin-film PV technologies primarily due to the success of First Solar, which utilizes CdTe technology." [5]

c. Concentrating PV

Concentrating photovoltaics (CPV) technologies use mirrors or lenses to concentrate sunlight (from 2 up to 1,200 times) onto high-efficiency silicon or multijunction (MJ) PV cells. “The CPV use concentrating optics made out of materials such as glass, steel, and plastic to focus sunlight onto a relatively small semiconductor area. Recent improvements to MJ PV cells have produced cell efficiencies of 43.5% in the laboratory.” [5] The use of CPV systems for utility-scale electricity generation is expected to grow.

d. Emerging PV Options

A number of other PV technologies, frequently referred to as third-generation PV, are being developed. A couple of examples from this category are the: dye-sensitized and organic PV solar cells. Dye-sensitized solar cells use dye molecules absorbed onto a nanostructured substrate and immersed in a liquid or gel electrolyte to absorb solar radiation and have demonstrated efficiencies as high as 11.1% during testing. “Organic PV (OPV) solar cells, based on polymers or small molecules with semiconductor properties, have demonstrated laboratory cell efficiencies above 8%; organic modules have the potential for low-cost manufacturing using existing printing and lamination technologies” [11].

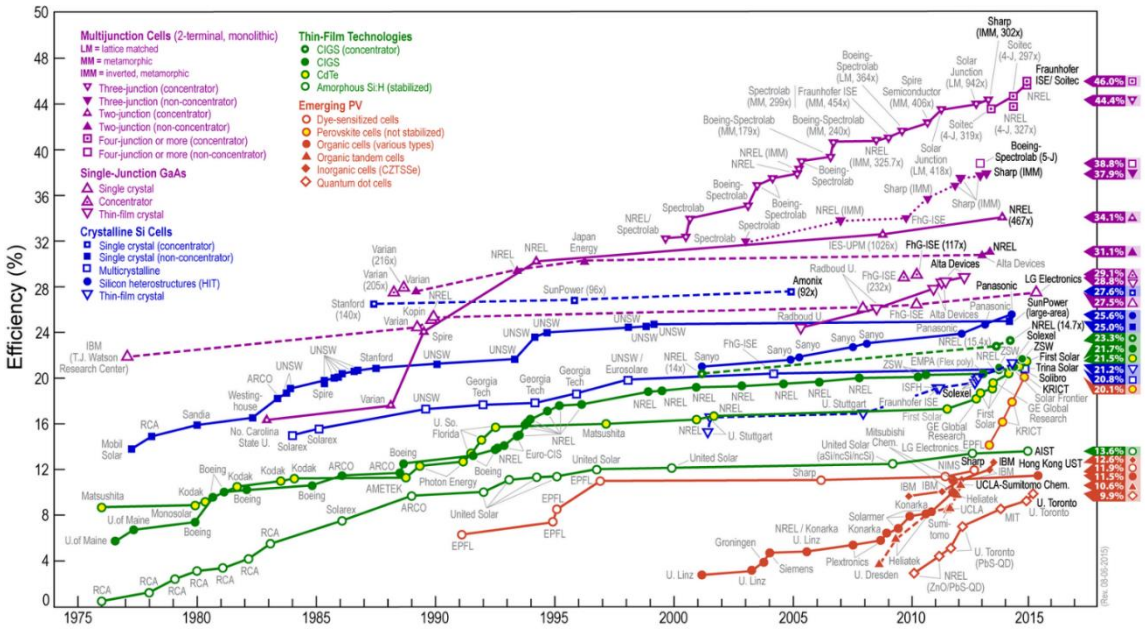

Figure 3: Laboratory best-cell efficiencies for various PV technologies [12]

PV Power Plant: A classification based on construction type.

In addition to the categorization of PVs by their respected module technology, they are also categorized by their size and structural environment. The main categories that account their modularity are: Open Air Plants, Flat Roof Plants, Pitched Roof Systems and Facade Systems. A brief analysis for each one of these categories can be found on the following sections.

- Open Air Plants: These plants are mostly large plants such as solar farms and range on the megawatt scale. The foundation of the overall structure is usually a long steel rod driven into the ground, which supports the rails that the PV modules will be nested.

The modules are fixed onto these rails with module clamps. The material for the module support structure is mostly aluminum or galvanized steel.

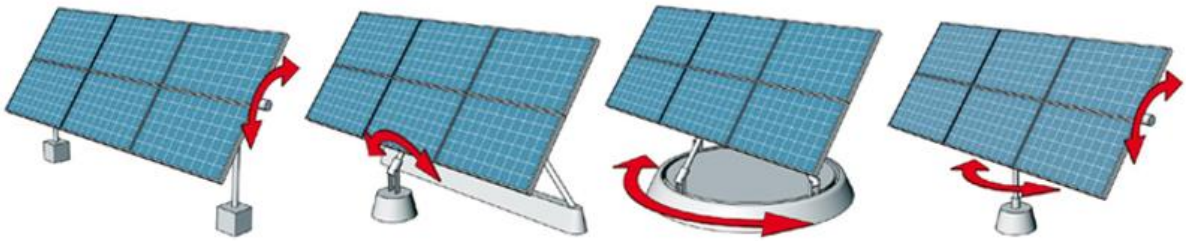

Figure 4: The four most common types of tracking systems [13]

An alternative the previous foundation is the screw-in foundation in which a spiral-shaped tube is screwed into the ground to ensure a secure support. If the ground is rocky or if construction must progress especially quickly, concrete foundations, are used. Another design consideration is that the individual systems should be erected at a proper distance from each other in order to prevent mutual shading when the sun is low in the horizon. Moreover, some open air plants are also built with solar tracking systems. The available options are the dual-tracker plants (dual-axis) and single-tracker plants (single-axis). The dual-axis technology provides a much greater yield but its mechanically complex design means a substantial price raise. Most plants use astronomic trackers in which the module always faces the sun. This is especially useful since sun's relative position changes throughout the year. Other plants use a brightness tracker, which locates brightness levels. This method can increase the penetration levels from sun's irradiance in the instance of a cloudy sky. During the shading generated

from the clouds the maximum irradiance might not be located on the sun's direction but rather on a spot in the sky that is not covered by clouds.

- Flat Roof Plants: These plants are located on flat roofs and have a couple of different supporting structures. One such structure, uses flagstones as the foundation for the PV supporting frames, which are usually made by aluminum. This method is implemented in order to avoid roof modifications and unnecessary drilling. Another alternative is to use polyethylene tubs weighed down with ballast (gravel, paving slabs, etc.) [14].

Figure 5: A tub and ballast mounting system by ConSole

The cabling of such as system passes through metal tubes which protect the conductors from harsh weather and possible mechanical stress. Alternatively, in the event that a roof that can only carry small area loads, the classic heavy-load foundation might be recommended upon further investigation. If that is the case then there are other systems that have less weight. These systems have an aerodynamic design that allows them to stay in position, as if they were mounted, under different weather conditions. The PV panels are pressed down on the ground by the wind from the front (south bound wind); or when

the wind blows from the back of the system, then openings on the top side cause a suction on the ground (north bound wind). Moreover, as all panels are interconnected, so there is a high degree of construction stability for the overall system (Figure 5).

Figure 6: Solution for roofs with low bearing capacity by LORENZ

- Pitched Roof Systems: Photovoltaic installations on pitched roofs are the most common form of PV systems and are found both in urban and rural areas. They are relatively cheap with a fast and easy installation since the roof provides a good foundation with a proper slope. There are two options within this category the erected systems and the in-roof systems. For the erected systems, a standard practice dictates that the panels keep a couple of tiles distance from the roof edges to avoid damages due to strong winds. The mounting of the module supports, consists of stainless steel roof hooks that are screwed to the rafters of the roof. A sufficient distance of the hook from the tiles is important, as the hook could bend with the weight of snow and damage the roof tiles.

Figure 7: An erected system installation on a pitched roof

The horizontally arranged rails are made of aluminum and are suitable for holding the connecting cables. The alternative to the erected photovoltaic system is the in-roof system that is integrated into the roof. Such an in-roof system (or roof-integrated system) consists of solar modules that form the actual roofing. A feature of this system is the combination with skylights and solar thermal collectors. When using the in-roof system, sufficient back ventilation of the plant must be provided otherwise the module temperature rises and the annual yield is less than a similarly arranged on-roof plant.

Figure 8: An in-roof system installation on a pitched roof

- Facade Systems: Facade systems are mostly installed on industrial or office buildings. The south oriented facade provides only about 70% of an optimally arranged solar system. However, there are further limiting effects on the annual yield: shading due to trees, fire escapes, other buildings, and so on. Since the facade system covers a part of the building it provides an extra layer of insulation from the environment. This can result in a 25-40% reduction of the energy consumed for indoor climate control.

Figure 9: A facade system on a municipal building in Madrid (Spain)

PV Power Plant: A classification based on energy management.

- Stand-alone PPP: These plants are not connected with the main power grid hence they rely on the system itself for its energy needs. The generation should ideally much the consumption; but this is very hard to manage since a lot of energy is consumed during nighttime. For this reason, an energy storage system has to be added. The energy storage system will store the excess energy generated during daytime and will dispatch it during nighttime when it is needed. Alternatively, the stored energy can be used during cloudy days too. These systems are most commonly used in remote locations where the power grid lines cannot reach.
- Grid Interconnected PPP: In this case, the power plant is interconnected with the main grid and can inject the generated energy when needed. These plants are becoming more common these days since many governments around the world provide incentives for such plants. Incentives come usually in the form of low taxes or partial project funding. Many utilities have these kind of systems solely for supporting their generation; either on distribution level (DG) or in a larger scale at a transmission level.

- Grid Interconnected PPP with Energy Storage**:** This type of system can operate as stand-alone or grid interconnected PPP on demand. This provides a lot of flexibility for the operator. The system can be used in support of the main grid or can be isolated thus creating an "island" that will be operated and controlled locally. These systems usually have a Battery Energy Storage System (BESS), which stores the

excess energy and will dispatch it based on optimal operating criteria. The PPP shares a DC bus with the BESS that minimizes the capital cost, since only set of inverters will be utilized for both systems. A similar system will be used for this study and more details about that system will be presented in Chapter 4.

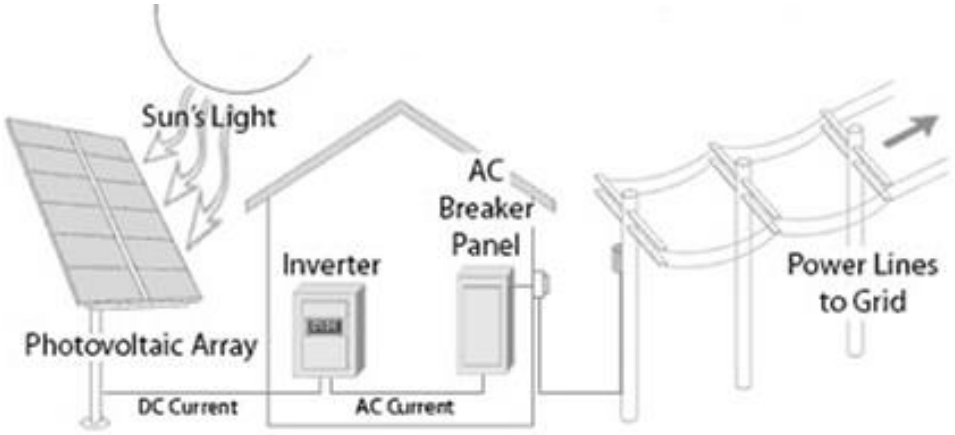

Figure 10: A typical residential grid interconnected PPP [15]

CHAPTER THREE

ENERGY STORAGE SYSTEMS

Pumped Hydroelectric Energy Storage

Pumped Hydroelectric Storage (PHS) is one the most popular energy storage systems and is broadly used from many electric utilities around the world. The basic concept of the PHS relies on the exploitation of hydraulic potential energy. When an excessive amount of energy is generated, it is used to pump water to an upper reservoir, which is located at a higher level. This usually happens during off-peak hours when the energy price is low. The opposite process takes place when the load is peaking. At that point, the stored water is released through the reversible pump-turbines to generate electricity thus satisfying the load demand. Sophisticated control systems allow the PHS system operator to release the water through the penstocks, when needed, onto the lower reservoir through turbines that move electricity generators. A typical PHS usually consist of the following parts: an upper reservoir, penstocks, waterways, a reversible pump/turbine, a motor/generator, gantry cranes, transformers, and a lower reservoir (Figure 11).

The first PHS units were installed on several manufacturing plants in Italy and Switzerland around the late 19th century in order to store excess energy generated by their power stations during the night. This energy will eventually be used to serve their load needs during the following day. In time, PHS stations were accepted as a common practice by a number of European countries (early years of the 20th century) and were used in the

optimization of economic dispatch of thermal power plants. The roundtrip efficiency of a modern PHS system is typically around 70–85%. [16]

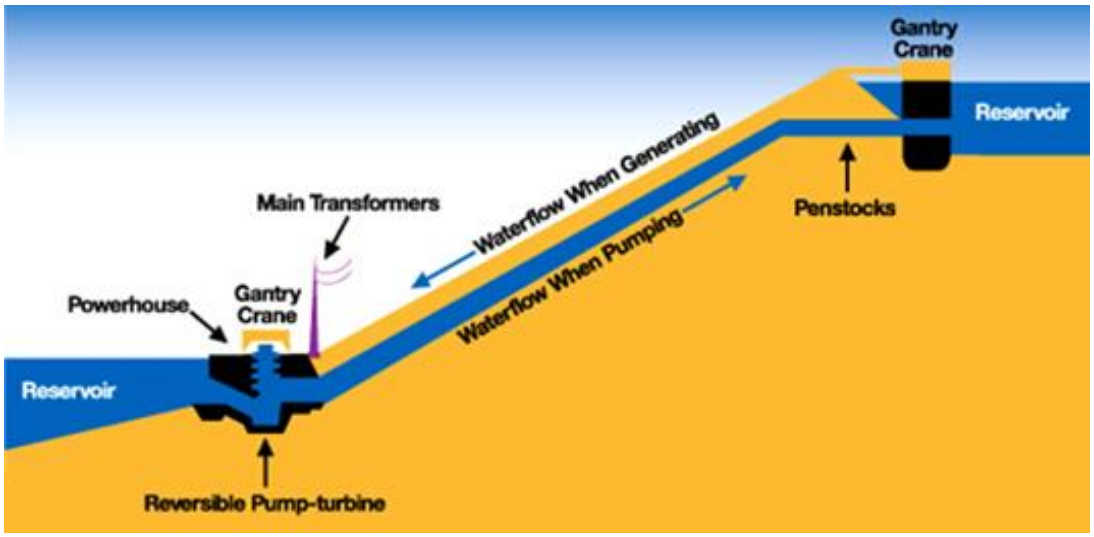

Figure 11: The Ludington PHS plant sits on a 1,000-acre site along the Lake Michigan shoreline [17]

Compressed Air Energy Storage (CAES)

A Compressed Air Energy Storage (CAES) systems uses the energy from the power grid to pressurize air into a (usually) underground reservoir. The compressed air is then released through a turbine for power generation when energy need rises. A typical CAES comprises of a motor/compressor, an air reservoir, a recuperator, a turbine and a power train motor/generator as illustrated in Figure 12.

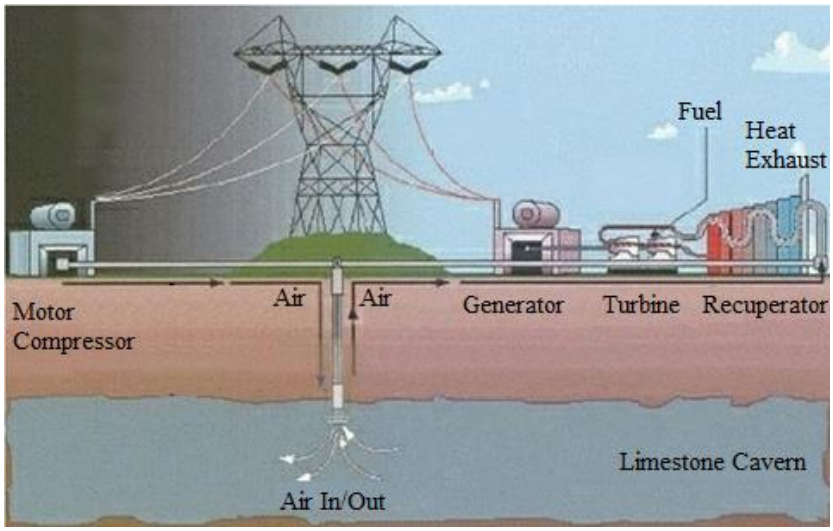

Figure 12: An illustration of a diabatic CAES system [18]

On a CAES, when air is released, it flows into the expander combustion train which produces the electricity. A lot of research is being conducted that aims to improve the efficiency of such a CAES.

One standard method, called the diabatic method, is to release the air, from the high-pressure storage cavern, through the recuperator with the purpose of preheating the air going to the turbine. While the most efficient method, called the adiabatic method, returns the heat generated at the turbine back to the recuperator to heat the colder air, which just reached the recuperator. The adiabatic method, creates higher air pressure while the heat losses of the system are minimized. Moreover, this type of CAES contains small inlet air heaters that keep the expander and the recuperator warm for a fast response to full load [19].

Common places that reservoirs are located are salt caverns, an abandoned hard-rock mines, depleted gas fields, or aquifers. All the previous places are the most economical method since no construction is involved. Alternative solutions would be, constructed underground storage caverns that have a rubber or steel layer along with a concrete lining to contain the air.

The average round-trip efficiency for typical CAES facilities ranges between 75% and 80%. The modern solutions achieve 85% and above efficiency. The charge/discharge ratio on these systems can vary greatly as the charging rate depends on the size of the compressor, the reservoir size and the reservoir pressure as compared to the generators power output.

CAES technology started in the early 1960s, during the early stages of gas turbine technology for electricity generation. The technology gained traction, during the 1970s, with typical application being load-following and peaking shaving. The first unit was constructed in Germany in 1978, followed by another unit in the United States, completed in 1991. A couple of the reasons behind its popularity are its fast response and the operating flexibility. This is why many nuclear power facilities, that wished to improve their overall utilization rates constructed CAES systems auxiliary generation and energy storage.

Flywheel Energy Storage

Exploiting inertia and storing energy in the form of mechanical kinetic energy is the main concept behind the operation of a flywheel. In inertial energy storage systems, energy is stored in the rotating mass of the flywheel. A popular practice (involving a flywheel)

from the past can be found on the ancient craft of pottery, where with a kick on the lower wheel of the rotating table the energy would start a motion which was sustained for a duration of time. The rotating mass stores the energy input so that rotation could be maintained at a relatively constant rate.

The application of flywheels for longer storage time is much more recent and has been made possible by developments in technology that involves improved materials, advancements in bearing technology, etc. The energy stored on flywheels, as compared to their physical characteristics (size, weight), cost is very low, and their utilization was mainly associated to their major advantage of being able to deliver very a lot of power in a short burst of time. Flywheels are used with steam and combustion turbines as supportive system for power generation.

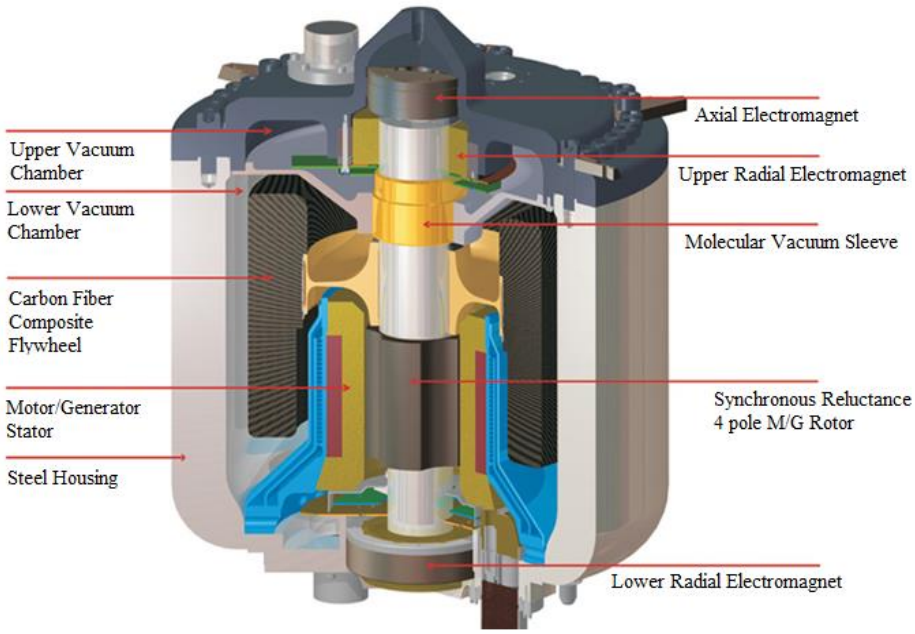

Figure 13: An illustration of the flywheel technology by PowerThru

While power electronics, vacuum housings and magnetic bearings become more popular, the round-trip efficiency of flywheel systems have been improved. Many current flywheel models have a round-trip efficiency around 70% to 80%, with some newer designs even higher [20].

Electrochemical Capacitors Energy Storage

Electrochemical capacitors (also known as Ultracapacitors) are quite similar to batteries as they have two electrodes immersed into an electrolyte, which is separated by a porous separator. They combine features from both technologies, having the energy storage capacity of a battery and the operating characteristics of a capacitor.

The energy is stored through the electrostatic charge, of opposite surfaces. The charge is developed between the electrodes and the electrolyte ions (Figure 15).

Since Ultracapacitors, move electrical charges between solid-state materials they can be cycled thousands of times at a very fast rate and at any level of discharge. These advantages are not available on chemical batteries as the chemical reaction restrains the response time as well as the depth of discharge [21].

The average DC–DC round-trip efficiency of an electrochemical capacitor is 80% to 95% during normal operation, with variations because of the multiple design types. Their total capacitance is directly related to the surface area of the electrode, hence the energy stored is proportional to the square of the applied voltage [22].

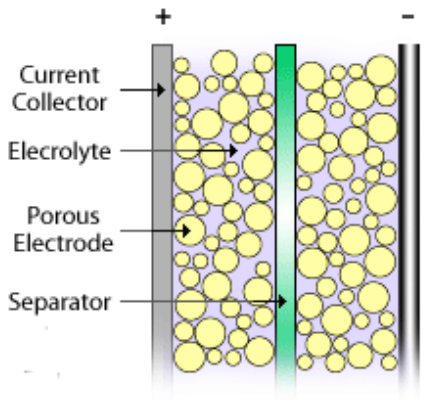

Figure 14: An Electrochemical Capacitor Cell

Ultracapacitors are sensitive to temperature and their lifecycle can be affected by abnormal temperature levels. The normal upper operating temperature of an electrochemical capacitor is typically 85°C. While in operation, the capacitor's internal temperature rises, hence the environmental temperature has to be controlled in a way that the internal temperature does not exceed 85°C. If that is not accomplished then the elevated temperatures will decrease the unit's life.

Electrochemical capacitors are a very promising technology. As a developing technology, there is a lot of room for improvement, main areas that heed attention are: increased operational capabilities, costs reduction and enhanced reliability.

Superconducting Magnetic Energy Storage

Superconducting Magnetic Energy Storage (SMES) systems, store energy in the magnetic field created by the flow of direct current in a coil of cryogenically cooled,

superconducting material (Fig. 3.5). A SMES system consists of a superconducting coil, a power conditioning system, a cryogenic refrigerator, and a cryostat/vacuum vessel that keeps the coil at a low temperature. Maintaining the coil at a low temperature is important in order to maintain its superconducting state, a state that allows energy storage at high efficiency levels.

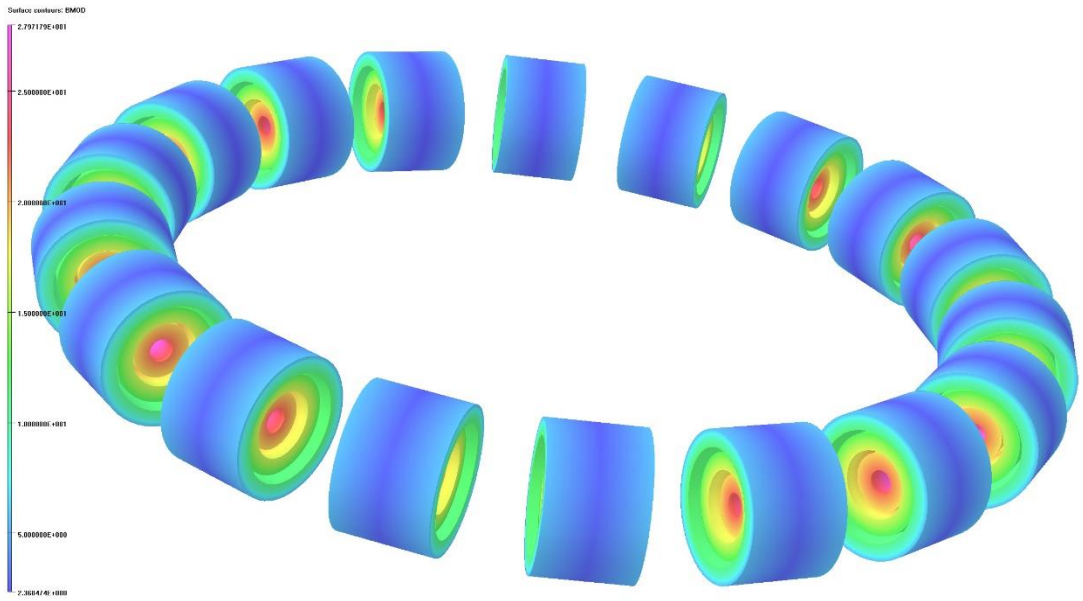

Figure 15: Magnetic field (in Tesla) superimposed over the SMES system consisting of several HTS coils [23]

These systems have a very fast response (few milliseconds) and can generate a lot of energy but only for short duration, in a similar manner as the flywheel. So they compete with flywheels in applications that require multiple, short interval discharges. Even though their cost is high when compared to other ESS technologies, their cost per unit of energy

stored is really competitive. It often the preferred equipment for Flexible AC Transmission Systems (FACTS) related applications or other transmission solutions. These systems are generally used to provide power-grid stability in a distribution systems and power quality at manufacturing units with critical loads highly susceptible to voltage instabilities.

Thermal Energy Storage

Developed almost three decades ago, Thermal Energy Storage (TES) systems are divided into three major groups: the Aquiferous low-temperature TES (ATES), the High-temperature TES (HT-TES) and the Cryogenic Energy Storage (CES).

One of the most common system of TES is the HT-TES, and more specifically the molten salt type. This type can be utilized as a thermal ESS that retains thermal energy collected by a solar tower or a Concentrated Solar Power plant (see Chapter 2) so that it can be used to generate electricity as needed (Figure 17). There are various molten salt mixtures; the most popular mixture contains sodium nitrate, potassium nitrate and calcium nitrate. This mixture is preferred as it is non-flammable, nontoxic and has already been tested in many different industries as a heat-transporting medium. The operating concept behind this technology is relatively simple, the hot salt is pumped to a conventional steam generator to produce steam which is then transferred on a turbine/generator. The turbine/generator combination used is similar to the ones used in any conventional coal, oil or nuclear power plant.

Similarly to the HT-TES, the ATES which relies on the storage and recovery of thermal energy underneath the surface of the earth. ATES systems are frequently used to provide heating and cooling for buildings, depending on the season and location. Storage and recovery of thermal energy is achieved by extraction and injection of groundwater from aquifers using groundwater wells. During summer, the groundwater pumped from underneath the earth's surface, is used for cooling purposes. That is achieved by discarding the building's heat onto the groundwater through a heat exchanger. Then, the heated groundwater is injected back into the aquifer, which creates a storage of heated groundwater. In wintertime, the flow direction is reversed such that the heated groundwater is extracted and can be used for heating.

Cryogenic energy storage (CES) uses low temperature (cryogenic) fluids such as liquid air or liquid nitrogen as an energy storage medium. External energy is used to cool atmospheric air down to -195 °C, where it liquefies. The liquefied air, takes up 1 thousandth of the volume of its former gas state and can be kept for a long duration of time in a large vacuum container at atmospheric pressure. When electricity demands rise, the liquid air is pumped at high pressure into a heat exchanger, which acts as a boiler. Air from the atmosphere at ambient temperature, or hot water from an industrial heat source, is used to heat the liquid and turn it back into a gas. This massive increase in volume and pressure is used to drive a turbine that generates the electricity needed.

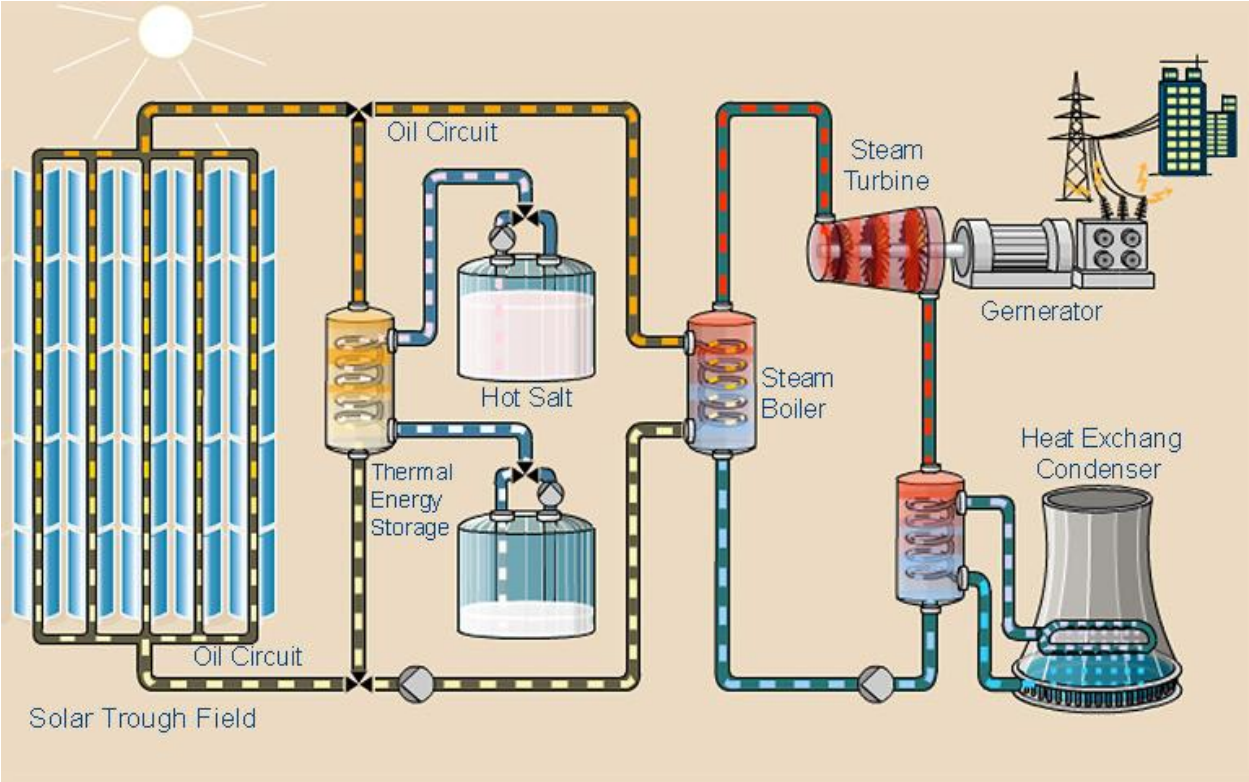

Figure 16: Schematic of a Parabolic Trough Power Plants (PTPP) with a High-temperature TES [24]

Battery Energy Storage

The most traditional of all energy storage devices for power systems is electrochemical energy storage (EES), which can be categorized into three groups: primary batteries, secondary batteries, and fuel cells. Primary and secondary batteries use their chemical components, while fuel cells have chemical energy supplied to them in the form of synthetic fuel (hydrogen, methanol or hydrazine). Unlike secondary batteries, primary batteries cannot be recharged when the built-in active chemicals have been used, and therefore strictly they cannot be considered as genuine energy storage. The term ‘batteries’,

therefore, will only be applied for secondary batteries. Batteries and fuel cells comprise two electrode systems and an electrolyte, placed together in a special container and connected to an external source or load. A typical BESS consists of battery modules, a Power Conversion System (PCS) and a transformer, which is usually located at the Point of Common Coupling (PCC) as, illustrated in Figure 17.

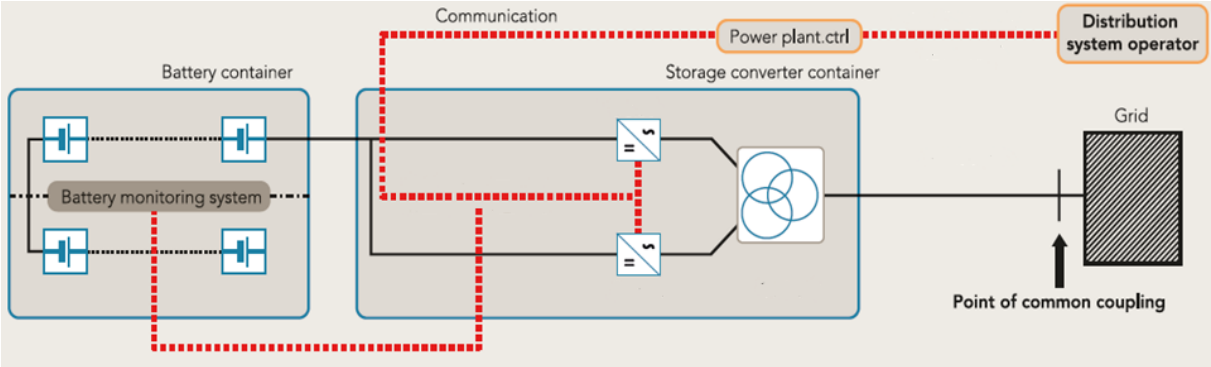

Figure 17: An illustration of a typical Battery Energy Storage System

These two electrodes, fitted on both sides of an electrolyte and exchanging ions with the electrolyte and electrons with the external circuit, are called anode and cathode. As anode, we define the oxidizing electrode, which is, the electrode that is sending positive ions into the electrolyte during discharge. When supplying positive charges to the electrolyte, the anode itself becomes negatively charged and therefore can be considered as an electron source. At the same time, the cathode consumes electrons from the external circuit and positive ions from the internal circuit. To maintain electric current in the external circuit, electrons have to be generated at the anode and used up at the cathode. The

electromotive force, of a battery, which initiates the electric current, is the difference between the electric potential of the electrodes. The terminal voltage equals the electromotive force minus the voltage drop in the battery due to its internal resistance, which contains frequency and time-dependent components associated with the electrolytic processes, ohmic resistance against the charge transport in the entire internal circuit components, an external load dependence component, and the remaining energy contents of battery component. The smaller the value of internal resistance the lighter is a battery's turnaround efficiency, since there is a linear dependence between thermal losses in a battery and its internal resistance. High reaction rate and good transport conditions will lead to a substantial decrease in the irreversible thermal losses in any electrochemical battery. Both factors can be met by working at high temperatures and with chemically active electrodes. In both cases, the electrolyte will be a limiting factor owing to problems of stability and transport properties. The use of ceramic materials, which have a suitably high specific conductivity for ions, is a promising possibility. The development of these so-called solid-state ion conductors has contributed to a breakthrough in battery technology. [16]

Table 1: Major BESS project implemented in USA

Name	Type	Rated MW x hrs	Location
Notrees Wind Energy Storage Project	Advanced Lead Acid	36 x 0.25	Texas
Laurel Mountain	Lithium Ion	32 x 0.25	West Virginia
Golden Valley Cooperative Project	Nickel Cadmium	27 x 0.25	Alaska
Primus Power Modesto	Zinc Chlorine Redox Flow	25 x 3	California
Anchorage Area BESS	Lithium Ion	25 x 0.6	Alaska
Johnson City	Lithium Ion	8 x 0.25	New York

Flow Batteries

"Flow batteries store and release energy through a reversible electrochemical reaction between two electrolytes." [21] There are four types of flow batteries currently in production or in very late stage of development: vanadium redox, zinc bromine, polysulfide bromide, and cerium zinc. Flow batteries are typically made from three subsystems (cell stacks, electrolyte tank system, and control system) plus the PCS system. The power and energy ratings of the flow battery are independent of each other. Polysulfide bromide systems are designed at a system level, requiring specific arrays of cell stacks for the particular power rating desired and specific storage tank size for the energy rating desired. Zinc bromine and cerium zinc manufacturers have settled on modular units with fixed power and energy capacities, respectively. Due to their modular design, increasing the

capacity of the systems requires discrete units of power and energy capacity. Vanadium redox manufacturers have designed a system using both strategies. During operation, the two electrolytes flow from the separate holding tanks to the cell stack for the reaction, with ions transferred between the two electrolytes across a membrane; after the reaction, the spent electrolytes are returned to the holding tanks. During recharging, this process is reversed. As this technology is highly flexible both in its physical makeup and its activity potential it is able to support a wide variety of applications in markets including transmission, retail, and renewable energy. [21]

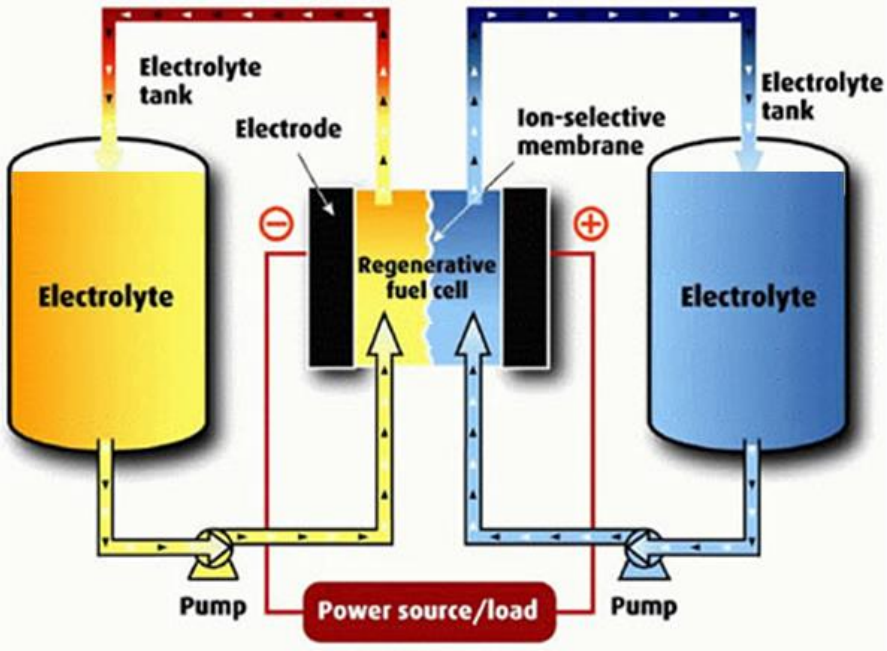

Figure 18: An illustration of a typical Flow BESS [25]

Sodium Sulfur Battery

The sodium sulfur battery's (NAS) battery cell is a cylindrical electrochemical cell with a molten-sodium negative electrode in the center and a molten-sulfur positive electrode on the outside, separated from the negative electrode by the β-alumina solid electrolyte (Figure 19). When a cell is discharged, sodium at the negative electrode discharges electrons, and sodium ions pass through the β-alumina electrolyte to the positive electrode, where they react with sulfur to form sodium polysulfide. Vice versa, when a cell is charged, this reaction is reversed.

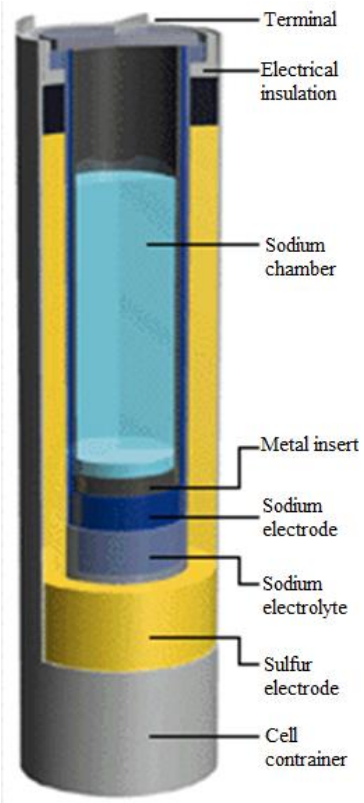

Figure 19: An illustration of a typical Sodium Sulfur battery [26]

The sodium polysulfide at the positive electrode decomposes, and sodium ions return to the positive electrode. The average round-trip efficiency is 89% for the storage module. Prospects for this technology are promising in the retail market for energy management and power quality. One significant benefit of this technology is its ability to provide output in either a long-term or short-term mode.

Lead-Acid battery

Lead-Acid (LA) battery technology research has been ongoing for more than 140 years. The two predominant types of LA batteries are flooded (or vented) and valve regulated (or sealed). Flooded lead-acid batteries are used in three applications: starting and ignition, deep cycle, and industrial uses, while VRLA are used in applications such as industrial tools and backup power. The electrodes in LA batteries are used both for part of the chemical reaction and for storing the results of the chemical reactions on their surfaces. Therefore, both the energy storage capacity and power rating are based on the size and geometry of the electrodes. Because of their low cost and reliability, LA batteries remain a favorite for a wide variety of market applications in the transmission, retail, and renewable energy markets. Although the possibility exists to use them in a variety of applications, environmental and operational effects curtail the list of applications truly available to them. However, LA batteries will remain an important energy storage technology in a number of existing market applications for the near future; they will always be the low-cost option for less-taxing applications in the UPS, telecommunication, and remote/off-grid renewable markets.

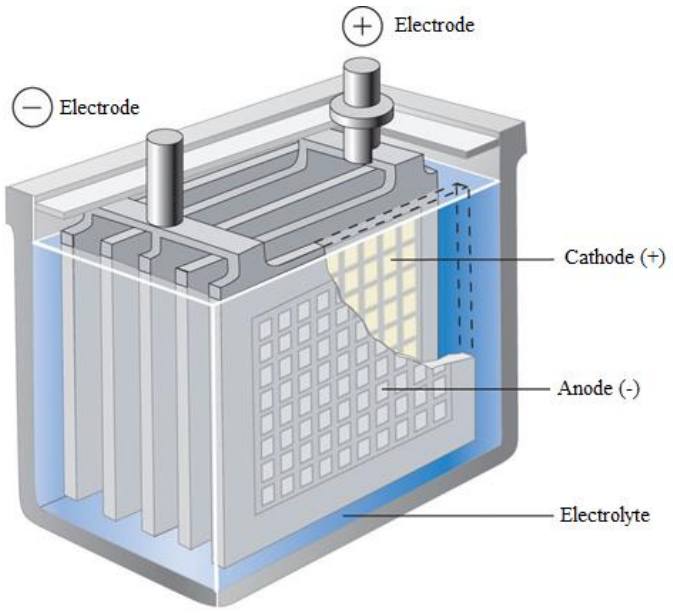

Figure 20: An illustration of a typical Lead-Acid battery [27]

Advanced Lead-Acid Technologies

"While developers of lead-acid technologies are improving the capability of conventional lead-acid technologies through incorporation of carbon in one or both electrodes, manufacturers such as GS Yuasa and Hitachi are taking other approaches. Advanced lead-acid products from these manufacturers focus on technology enhancements such as carbon-doped cathodes, granular silica electrolyte retention systems, high-density positive active material, and silica-based electrolytes. Some advanced lead batteries have supercapacitor-like features that give them fast response, similar to flywheels or Li-Ion batteries." [19]

Nickel Cadmium Battery

Swedish scientist Waldmar Jungner developed the first nickel cadmium (NiCd) battery (the pocket-plate style) in 1899. Three designs dominate nickel-cadmium battery design: pocket plated, sintered plated, and sealed. A typical design of a NiCd can be seen in Figure 23. Pocketplated NiCd batteries are used extensively in markets such as industrial and standby power, where durability is important. Sintered NiCd batteries dominate in markets such as for starting aircraft and diesel engines, where high energy per weight and volume are important. Finally, sealed NiCd batteries are used commonly in commercial electronic products, where lightweight, portable, and rechargeable power is important.

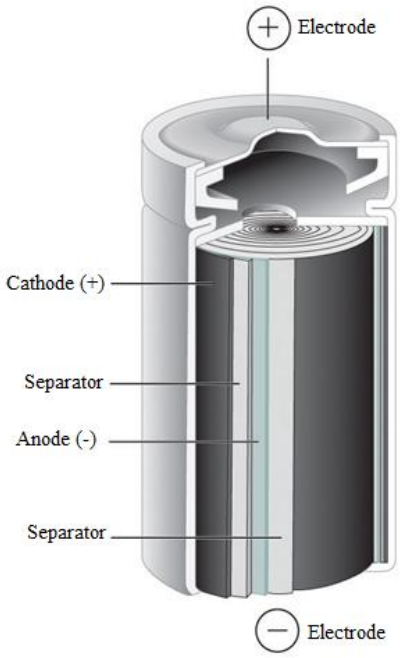

Figure 21: An illustration of a typical Nickel Cadmium battery [27]

The reliability of NiCd batteries makes them a favorite for a wide variety of market applications in the transmission, retail, and renewable energy markets. For many reserve power applications, NiCd batteries are one of the least expensive energy storage technology choices for most applications in the retail and some transmission applications. Nickel-cadmium batteries will remain an important energy storage technology in a number of existing market applications for the near future. Although slightly more expensive than LA batteries, their operating capabilities and excellent reliability span a wider operations envelope and longer cycle life, allowing for lower ownership costs.

Lithium-Ion battery

In the past few years, Li-Ion battery technology has emerged as the fastest growing platform for stationary storage applications. “Already commercial and mature for consumer electronic applications, Li-Ion is being positioned as the leading technology platform for plug-in hybrid electric vehicles (PHEVs) and all-electric vehicles. The most common types of liquid Li-Ion cells are cylindrical and prismatic cell. They are found in notebook computers and other portable power applications. Another approach, prismatic polymer Li-Ion technology, is generally only used for small portable applications (cell phones, tablets, etc.).” [21] Compared to lead-acid batteries, Li-Ion batteries are relatively new. There are many different Li-Ion chemistries, each with different characteristics. Large-format prismatic cells are currently under development.

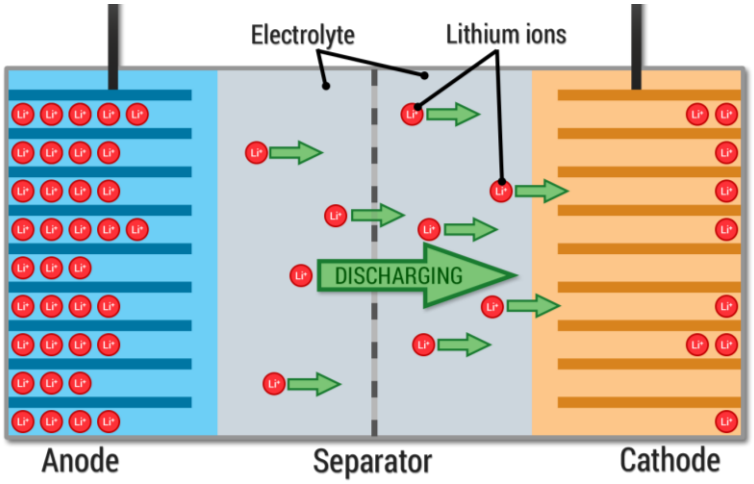

Figure 22: An illustration of a typical Li-Ion battery [28]

"A Li-ion battery cell contains two reactive materials capable of undergoing an electron transfer chemical reaction. To undergo the reaction, the materials must contact each other electrically, either directly or through a wire, and must be capable of exchanging charged ions to maintain overall charge neutrality as electrons are transferred. A battery cell is designed to keep the materials from directly contacting each other and to connect each material to an electrical terminal isolated from the other material's terminal. These terminals are the cell's external contacts." [19] Inside the cell, the materials are ionically, but not electronically, connected by an electrolyte that can conduct ions, but not electrons. "This is accomplished by building the cell with a porous insulating membrane, called separator, between the two materials and filling that membrane with an ionically conductive salt solution." [19] Thus, this electrolyte can serve as a path for ions, but not for electrons. When the external terminals of the battery are connected to each other through a load, electrons are given a pathway between the reactive materials, and the

chemical reaction proceeds with a characteristic electrochemical potential difference or voltage.

Energy Storage Technologies Overview

The technical maturity of the EES systems is shown in Figure 23. There are five maturity levels; mature, deployment, demonstration, development and research. Most ESS fall into the deployment category which essentially means that they have passed the demonstration stage but need more testing in order to reach a mature level.

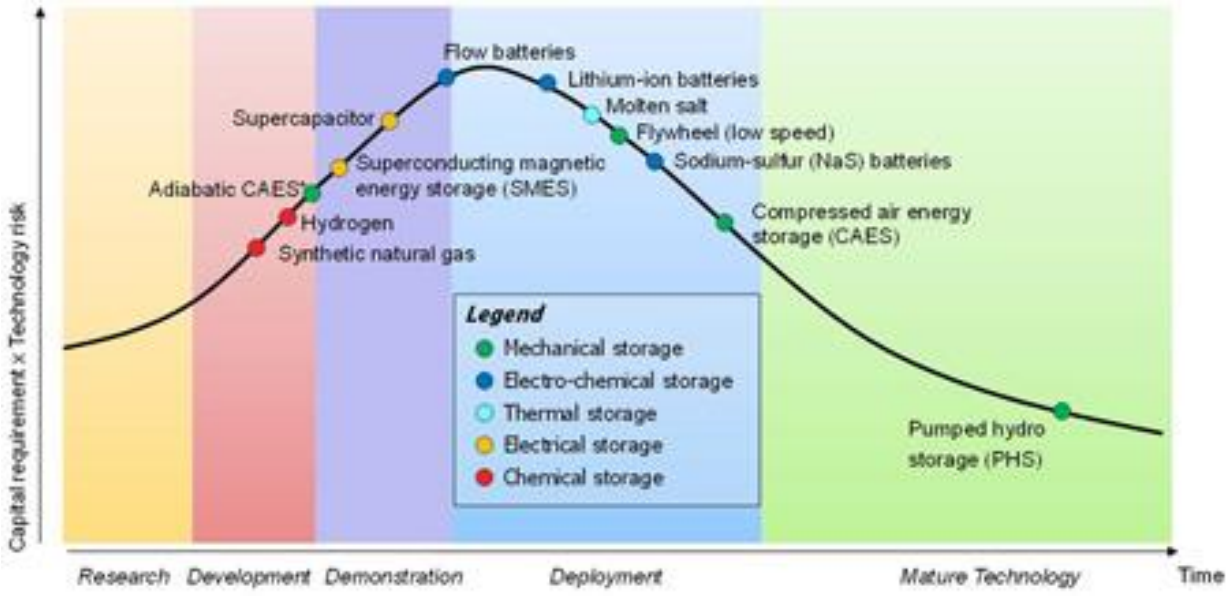

Figure 23: Energy Storage Technology Maturity Curve [29]

The PHS and the CAES (compressed air) systems could be considered mature which in only natural since they are the one of the oldest systems to be utilized for power

systems applications. More research is needed for the CAES (adiabatic), the Hydrogen (fuel cells) and the Synthetic Natural Gas which are relatively newer technologies. Maturity can be reached when the performance of the ESS is stable with good roundtrip efficiency and low cost.

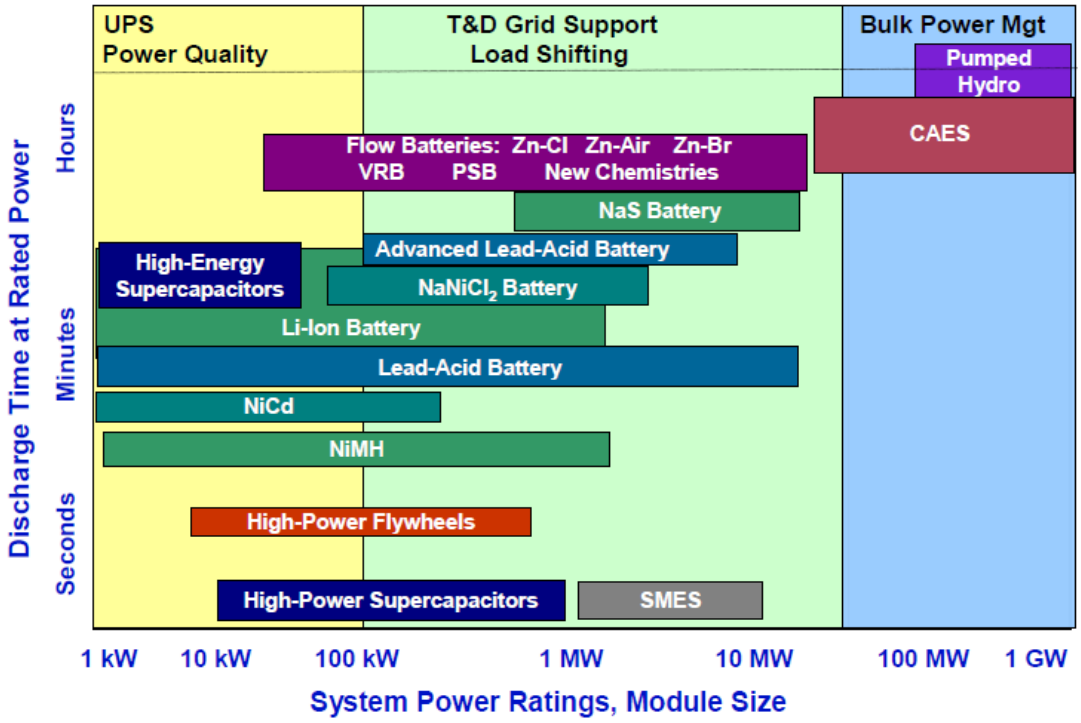

Figure 24: Sizing the different Energy Storage Technologies [19]

In [19] ESS are sized based on the application they are intended to support and in [30] the size and the application are correlated with a monetary value. These applications are usually referred as benefits that are provided by the ESS. Each benefit represents a discrete use of the ESS that can be quantified and valued.

Due to the currently high installation capital costs of most energy storage systems, the user must be able to utilize multiple applications/functions across different parts of the energy value chain, an aggregation of complementary benefits known as “stacking”. This concept is illustrated in Figure 25 for many of the energy storage functions served by the key applications. In Figure 24 and Figure 26 the characteristics of various ESS in terms of system power rating along and the duration of discharge at rated power are presented.

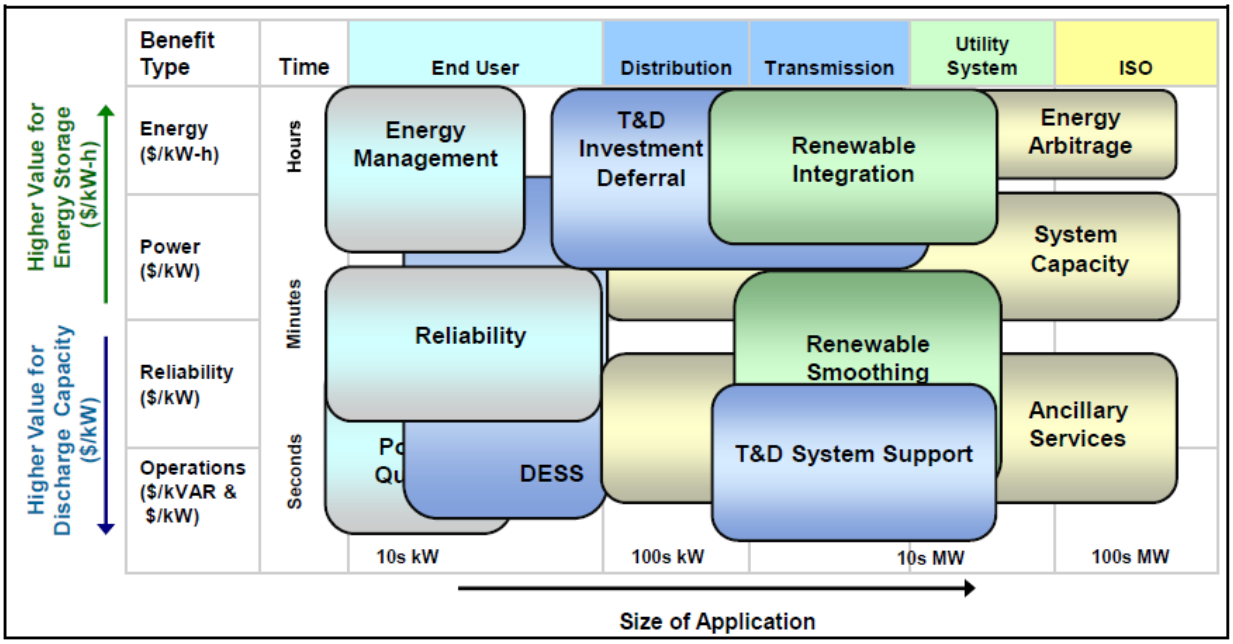

Figure 25: Operational Benefits Monetizing the Value of Energy Storage [30]

The monetary value presented in Figure 27 is a very rough approximation, since the accurate evaluation of the revenues introduced by an ESS is a fairly complicated

problem. This problem will be discussed and analyzed in detail in Chapter 4, where a case study for Advances Lead-Acid BESS will be evaluated.

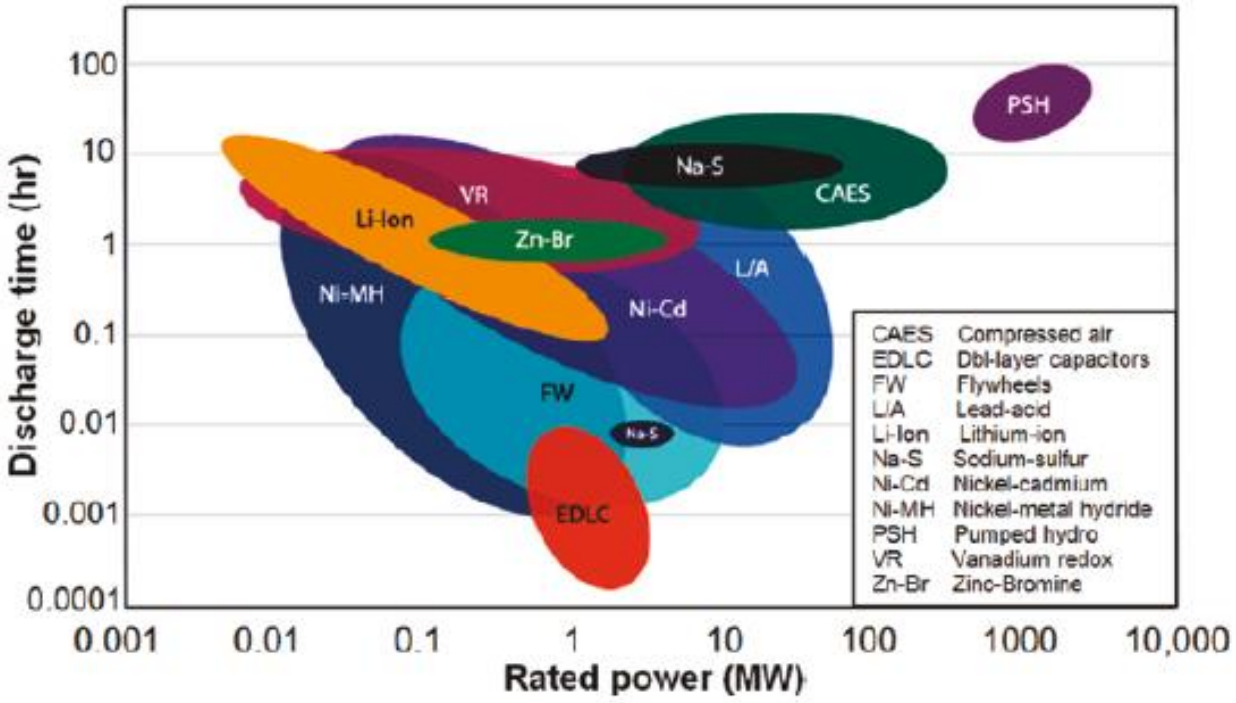

Figure 26: Comparison of Power and Discharge Time for Various Energy Storage Devices [31]

CHAPTER FOUR

BATTERY ENERGY STORAGE SYSTEMS: A FINANCIAL EVALUATION IN MICROGRIDS

Energy storage systems and more specifically Battery Energy Storage Systems (BESS) have been studied extensively for many different reasons [32]. Recently many researchers recommend them as a remedy to the variability and volatility of Renewable Energy Sources (RES) [33] - [36]. Regardless of the application a BESS supports the main components that such a system consists of, are the same. A typical BESS includes an interconnection with the grid, a power conversion system and batteries cells [37]. The power conversion systems, converts electricity bidirectionally, i.e. from the power source to the batteries (AC to DC) and from the batteries to the load (DC to AC) with high efficiency up to 95%. Moreover, a power conversion system can support the system by controlling, besides the real power, its reactive power too.

Many different types of batteries have been developed and more are being developed as research progresses. The technology keeps improving, which has resulted in batteries with high roundtrip efficiency (up to 90%), increased lifecycle, and reduced cost. The distinction between these different types of batteries is based on the technology and the different electrochemical components (electrodes, electrolytes, etc.). Some of the most

popular battery types used for BESS systems are: Advanced Lead-Acid, Lithium-Ion, Sodium-Sulfur, Zinc/bromine, Vanadium Redox, Sodium-Ion, Sodium Sulfur, etc. [38]

Advanced lead-acid systems have been used in many projects, since 2011. Innovation in materials is improving their lifecycle and durability. Several advanced lead-acid technologies have been developed while others are in pre-commercial and early deployment phase. These systems are being developed for peak shaving, frequency regulation, wind integration, photovoltaic smoothing and automotive applications [39]. Some advanced lead-acid batteries have features similar to supercapacitors, that give them really fast response almost comparable to flywheels [40].

The advantages of the advanced lead-acid battery are its: mature battery technology, low cost, high-recycled content and good battery life. Some of its disadvantages are: limited depth of discharge, low energy density, large footprint, and electrode corrosion limits useful life [20].

Due to the nature of their design, BESS can support many different RES related applications; such applications are: RES Time-shift, RES Capacity Firming and Wind Generation Grid Integration (Short/Long Duration), etc. Besides the above mentioned applications, a BESS can also support standard daily grid operations; such as: Electric Supply Capacity, Area Regulation, Electric Supply Reserve Capacity, Voltage Support, Transmission Congestion Relief, etc. [41].

Since the ultimate goal, of every operator, is to fully utilize every asset of the system, while maximizing the revenues, it is desirable for a BESS to support more than

one applications. These applications can be chosen based on the synergy level they have with each other. For instance in [41], we can find such a synergy matrix where all the possible applications are evaluated with regards to their compatibility and possible coordination. A higher level of synergy corresponds to a smother coordination between the different applications.

Upon choosing the applications that a BESS will support and while attempting to maximize the benefits obtained from it, optimal scheduling has to be pursued. Conceptually, an optimal scheduling scheme might sound straightforward, but in reality there are several factors that dictate the rules of such a process; which increase the complexity of it.

For this study, the synergy matrix in [41] was used as a guide and four applications were chosen, due to their high level of synergy with each other. These applications are: RES Time-Shift, RES Capacity Firming, Electric Energy Time-Shift and Electric Supply Capacity. The first two applications were used in order to support the operation of a Photovoltaic Power Plant while for the microgrid case all applications where coordinated and optimality was targeted.

Upon choosing the applications to be supported the optimal scheduling scheme has to be deployed. For this study the means to obtain such a scheme was through the utilization of two different algorithms. For the Photovoltaic Power Plant case, Mixed Integer Linear Programming (MILP) was used while for the microgrid case, Linear Programming (LP) was used [42]. The Photovoltaic Power Plant case was formulated as a MILP problem and

was solved as an np-hard problem [43]. While LP problem formulation was used for the microgrid case and was solved as a weakly polynomial time problem. Both algorithms provide the optimal solution.

Optimal scheduling

Photovoltaic Power Plant optimal scheduling

During the planning stages, the transmission lines and other related equipment are appropriately sized based on the PV plant. Hence, by limiting the output at the Point of Common Coupling to acceptable levels, BESS and PV can be analyzed separately from the rest of the grid. A simplified system as illustrated in Figure 27 is used for the study of the Photovoltaic Power Plant support. Assuming that the Photovoltaic Power Plant already existed, while the BESS is the new addition, this subsection aims to study how it could be supported the operation of such a power plant.

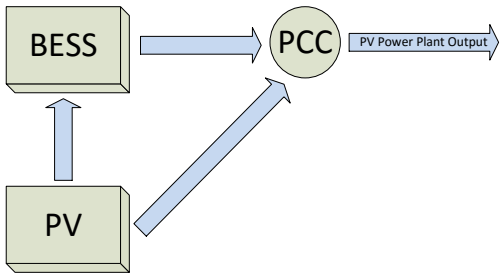

Figure 27: A BESS supporting the operation of a PPP

The optimization aims to limit the output variation at the Point of Common Coupling as seen by the grid while maximizing profit. That can be accomplished by firming the capacity of the PPP and dispatching energy when additional energy is in demand. Firming the capacity of a PPP increases its capacity credit. A lower capacity credit might be a result of many reasons, such as: suboptimal and fixed panel orientation, regular dust accumulation, shading by surroundings, high ambient temperature and high level of cloudiness. Hence, by exploiting the benefits of a BESS the capacity credit of the PPP can be improved. Moreover, since the target of the optimization is also to maximize revenue generated by the PPP, the stored energy is dispatched when energy prices are peaking.

Considering all the factors mentioned above, the problem is formulated as a Mixed Integer Linear Programming problem. The objective function for this case is given by:

$$f(x) = \max[({C_1}^T \cdot P_{PCC}) \cdot \Delta t] \quad (1)$$

Equation (1) combines the energy price with the power output at PCC. Hence, if (1) is successfully maximized, the optimization will be completed and the maximum revenue will be obtained while conforming to the power and energy constraints. The optimization is achieved by the use of the following equations which describe the system's behavior. The total power at the point of common coupling is used as the first equality constraint and is described in (1), for time-step *t*.

$$P_{PCC}(t) = P_{PV}(t) + P_{Bat}(t) \Rightarrow \qquad P_{PCC}^t = P_{PV}^t + P_{BatD}^t - P_{BatC}^t \quad (2)$$

The energy stored in the BESS is used as the second equality constraint.

$$E_{Bat}^{t} = E_{bat}^{t-1} - (P_{BatC}^{t} \cdot \Delta t) \cdot \eta_1 + (P_{BatD}^{t} \cdot \Delta t)/\eta_2 \quad (3)$$

The equations (2) and (3) form the set of the equality constraints for this problem. The inequality constraints are described as follows:

$$-\varepsilon \leq dP_{PCC} \leq \varepsilon \quad (4)$$

$$P_{BatC} \leq P_{BatMax} \cdot \beta \quad (5)$$

$$P_{BatD} \leq P_{BatMax} \cdot (1 - \beta) \quad (6)$$

ε dictates the smoothness level of the output of the system. The smaller the value of ε the smoother the transition between time steps. The variable β, is a decision variable which is useful to formulate the MILP optimization. The final two inequality constraints are derived from the BESS maximum power and energy and the following:

$$E_{Bat} \leq E_{BatMax} \quad (7)$$

$$P_{Bat} \leq P_{BatMax} \quad (8)$$

Microgrid optimal scheduling

On this subsection, the system under study is a microgrid and the illustration of it can be found on Figure 28. As it is obvious, the system, in addition to the components of Case A, has now a generator and a load. The new system is constructed this way in order to simulate a small grid in islanded mode (i.e. a microgrid). In this new updated scheme,

two additional applications are supported. These applications are: Energy Time Shift (ETS) and Electric Supply Capacity (ESC), as defined in [41].

The first application (ETS) aims to maximize the operational revenues by storing the excess energy generated by the generator and selling it when energy price is higher. The main difference between ETS and RES Time Shift is the energy source. The former uses a source the generator while the later use as energy source a renewable energy source, and in this case a PPP.

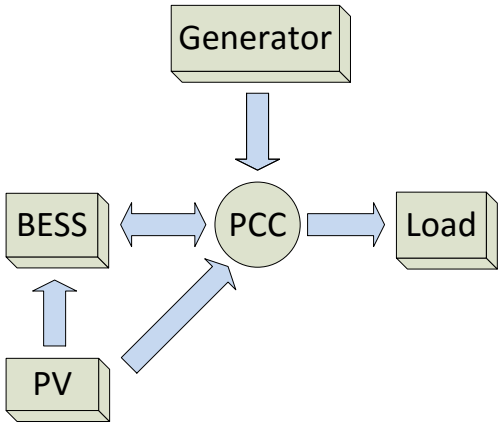

Figure 28: A BESS supporting the operation of a microgrid

The second application (ESC) has a financial impact through its cost avoidance nature. More specifically, the BEES is used as additional generation; thus supporting the generator. This way the generator uses less fuel and the rate of change in generation is kept on a more controllable scale. As it is obvious keeping the generation on specific region, results on a smoother operation of the generator, which leads on less “wear and tear” and

eventually reduced maintenance costs. Moreover, if desired the generator can be kept operating on a high capacity, close to its nominal values, which leads to higher fuel efficiency.

The objective function that will maximize the revenues for the microgrid scenario is:

$$f(x) = max[\, C_1^T \cdot (P_{BatD} - P_{BatC}) - C_2^T \cdot P_{Gen}) \cdot \Delta t] \quad (9)$$

In (9) the wholesale energy price is coupled with the power on the BESS. Similarly, the power at the generator is coupled with a fixed cost of operation. With (9) the revenues generated by the energy that the BESS discharges into the microgrid are maximized. In order to achieve the optimization, along with (3), a new equality constraint equation is created:

$$P_{Gen}(t) + P_{PV}(t) + P_{BatD}(t) = P_{BatC}(t) + P_{Load}(t) \quad (10)$$

Equation (10) essentially describes the desired real power equilibrium, between generation and demand at the PCC. Due to small size of the microgrid, real power losses on the distribution system are neglected. Furthermore, along with (7) and (8), a new set of inequality constraints is added into the problem formulation. The new inequality constraints are dictated by the generators ramp rate:

$$dP_{Gen} \leq \rho_1 \quad (11)$$

$$-dP_{Gen} \leq \rho_2 \quad (12)$$

Simulation Results and Discussion

Optimal scheduling and revenues

In order to simulate the PPP, Solar Power Data for Integration Studies were used. More specifically, this data, is synthetic solar photovoltaic (PV) power plant data points, from the United States from the year 2006. A dataset generated from the South Carolina region, is used for this study [44]. The wholesale energy price and load data used for this study, was obtained by Independent Electricity System Operator (IESO) of Ontario [45]. The data were in hourly intervals hence an extrapolation was applied in order to get the five-minute interval needed for this study.

Table 2: Test System Characteristics

Parameters	***Case A***	***Case B***	Parameters	***Case A***	***Case B***
BESS (MW)	39		Δt (min)	5	
BESS (MWhrs)	39		ε (MW/min)	0.2	-
η_1	0.90		$\rho_{1,2}$ (MW/min)	-	5
η_2	0.85		C1 ($/MWhr)	-	30
PPP (MW)	39		Gen (MW)	115	

The parameter values used for the simulations can be found on Table 2. The BESS was sized proportionally to the PPP. The efficiency levels used for the BESS correspond to the battery technology chosen for this case i.e. Advanced Lead-Acid. Usually, energy is

dispatched every 5 minutes from system operators hence for this study this time interval was used too. The generator was sized so it can serve the system in a peak time if needed. For the generator's given size an average cost of operation, which is 30$/MWhr, was used for the calculations. The ramp rate of 5MW/min is typical for the 115MW generator.

A sample from the results from the PPP case study is illustrated in Figure 29. The plots demonstrate the ability of the BESS to handle the PPP's variability. The output power, i.e. the power at PCC is now linear with a desirable rate of change. Also, after approximately 10^3 minutes and despite the fact that the PPP does not generate more energy (probably nighttime) the BESS dispatches its stored energy. This is justified because the energy price is increasing and the BESS tries to maximize the revenues.

For the microgrid case, the optimization worked in a similar manner as in case 1; but in this case BESS was supporting all four applications. In (13) the cost of operation without a BESS is calculated while in (14) the cost of operation with a BESS is calculated.

$$Cost_{without\ BESS} = [(P_{load} - P_{PV}) \cdot C_2 \cdot dt\ ] \quad (13)$$

$$Cost_{with\ BESS} = [(P_{Gen} \cdot C_2 \cdot dt) - (P_{BatD} + P_{PV}) \cdot C_1 \cdot dt] \quad (14)$$

Hence when subtracting (13) from (14), the result will be the revenue solely generated by the addition of the BESS. The revenues for a whole year were recorded and illustrated in Figure 30. In Figure 31, the revenues for a 12-year period are presented. A considerable variability in revenue is observed; that, has to do with the fluctuation of energy prices, PPP volatility and load variability.

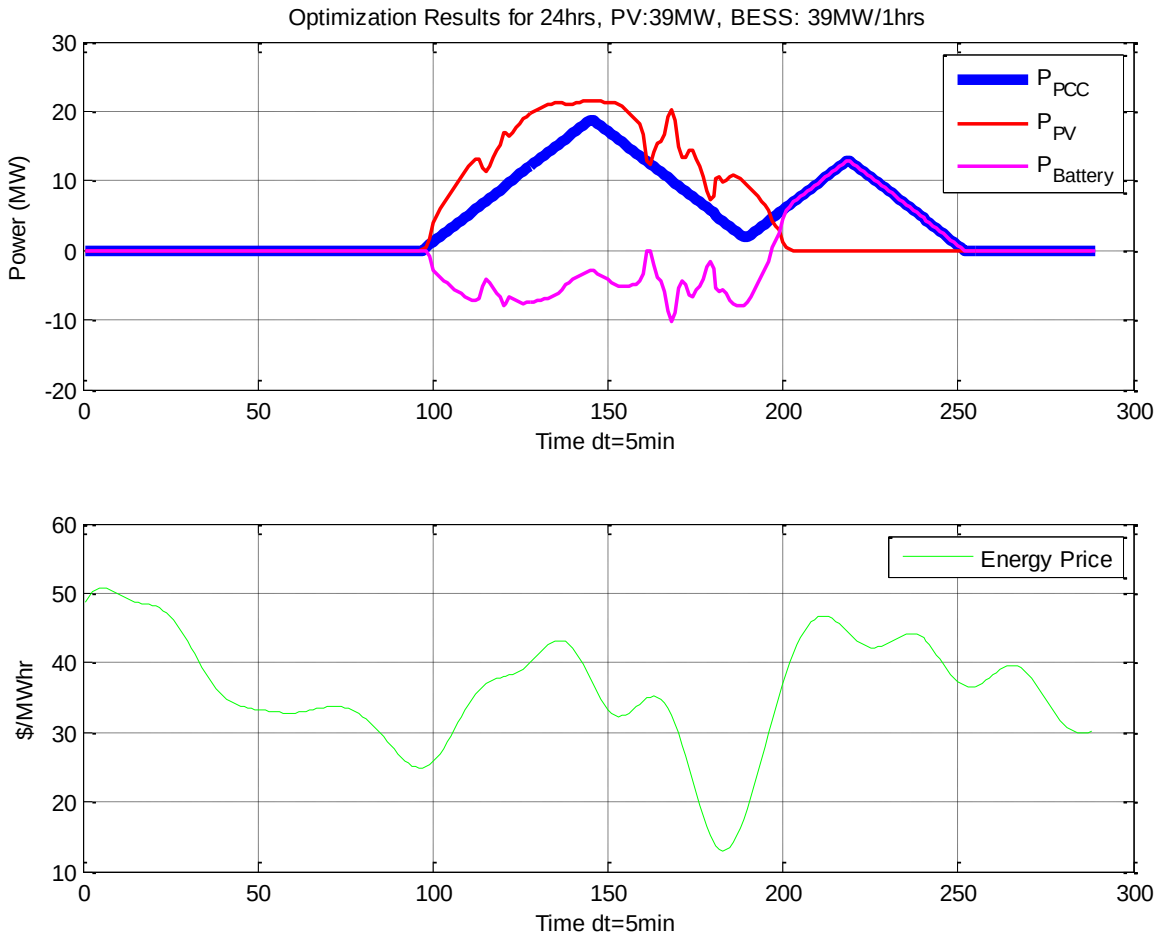

Figure 29: Sample of daily energy dispatch for the PPP case study

Besides the direct benefits mentioned above. There are additional benefits, these benefits come as a byproduct of the main applications and are usually referred as incidental benefits [2]. Such benefits are:

a) Reduced perceived transmission and distribution investment risk.

b) Dynamic operating benefits for the generator.

c) Reduced fossil fuel use.

d) Reduced air emissions from generation.

e) Operating flexibility e.g. respond better to changing circumstances.

f) Community energy storage increases system reliability, system security etc.

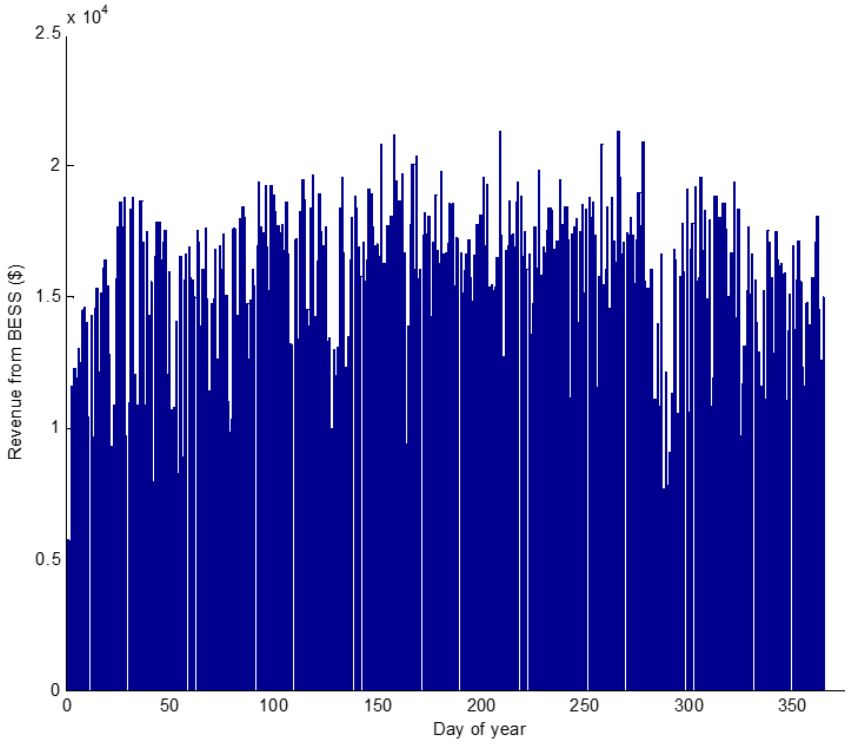

Figure 30: Sample of annual revenues per day for the microgrid case study

Financial analysis

In this section the financial analysis for the microgrid case is expanded. Since the revenue was calculated in the previous section, the next step is to calculate the corresponding cost and proceed in a cost/benefit analysis. The major cost of most projects

come in the form of the capex (capital expenditure). In this case the capex, is estimated $19.5 million (500$/MWhr); for a BESS with Advanced Lead-Acid batteries and sized as described in Table 2. A replacement of the battery modules after, approximately 4,500 cycles, for the price of $5,850,000 (estimated as 30% of the capex cost) is added to the costs. The batteries are fully discharged in every cycle and it is assumed that the capacity of the batteries will stay at a nominal value until they are replaced.

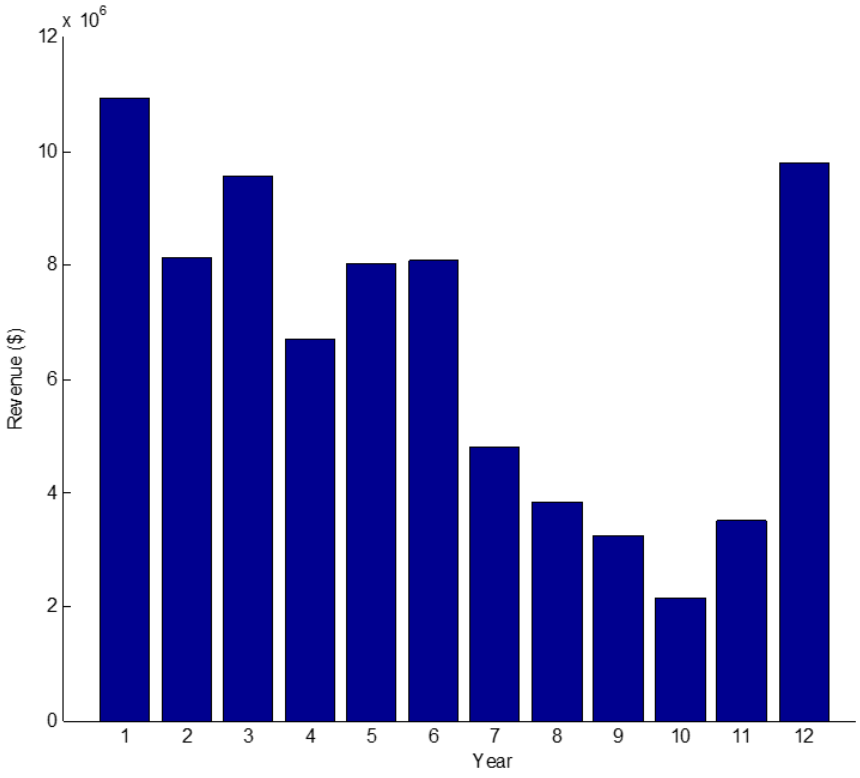

Figure 31: Annual revenues for a 12-year period

Moreover, there are annual fixed costs; which are $195,000 (e.g. labor associated with BESS operation, preventive maintenance). The variables costs (i.e. unscheduled maintenance and operation) depend on the number of cycles and are approximated at a cost of $17.81 per cycle. All the above costs were estimated based on data provided from [46] and [22]. There is no cost escalation throughout the 12-year period which to compensates the absence the energy price escalation for that period. Furthermore, the cost of capital used in this study is assumed to be 10% and this is the discount rate used [47]. Since the discount rate has a significant impact on the analysis, we present results for various discount rates ranging from 8% to 18%. Revenue estimations are presented in Table 3, along with variable costs, fixed costs and the final cash flow before taxes.

While following a similar approach to [47] and [41] an additional step is taken in this study; the present worth and discount factors are calculated and their impact is analyzed. To evaluate profitability, the Net Present Value of the project is estimated. The NPV is the present value (or present worth) at time zero of all cash flows (from the first year to the last year) minus the initial investment needed to undertake the project.

In addition, all cash flows are discounted at the cost of capital, which is the interest rate paid in order to borrow funds. Moreover, it is assumed that each year's cash flow are received around mid-year so we use mid-year discounting. More specifically we calculate Net Present Value as follows:

$$NPV = \sum_{i=1}^{12} \frac{CF_i}{(1+r)^i} - Investment \quad (11)$$

where CF_i is the cash flow in year i, r is the discount rate and *Investment* is the initial investment needed to undertake the project.

Table 3: The Financial Evaluation for a 12-Year Period

Year	Cycles	Revenue ($)	Fixed Costs ($)	Replacement Cost ($)	Variable Costs ($)
1	2,626	10,942,000	$19,500,000	-	46,776
2	2,292	8,139,500	$195,000	-	40,836
3	2,263	9,556,400	$195,000	5,850,000	40,311
4	1,933	6,708,500	$195,000	-	34,437
5	2,515	8,038,600	$195,000	5,850,000	44,801
6	2,366	8,089,300	$195,000	-	42,149
7	1,947	4,805,500	$195,000	5,850,000	34,686
8	1,172	3,835,500	$195,000	-	20,880
9	1,247	3,248,900	$195,000	5,850,000	22,216
10	856	2,145,000	$195,000	-	15,255
11	1,546	3,513,900	$195,000	-	27,536
12	2,405	9,787,800	$195,000	5,850,000	42,834

Using the projected cash flows presented in Table 3, the Net Present Value of the project is $12,295,126; which means this is a very profitable project. As it is obvious, if

there is a change in the assumptions these numbers can be influenced significantly. For example, if the cost of capital (discount rate) is higher, then the distant cash flow will have a significantly lower value.

Other factors that might affect the results are the variable costs; which in this study range from 0.3-1.7% of the revenues (depending on the year) but if in reality they were 2-3% of the revenues, this would change considerably the cash flows. In Figure 32, the NPV for three different scenarios is illustrated. These scenarios include the various discount rates and three different assumptions for the variable cost (actual, 5% of revenues, 10% of revenues).

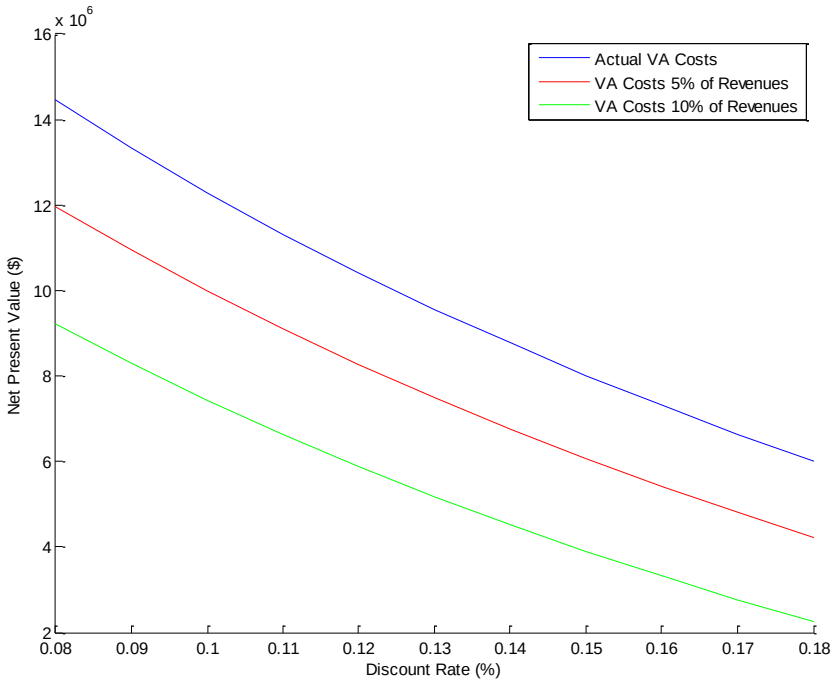

Figure 32: The Net Present Value profile chart.

Inspecting the revenue data for the 12-year period, found in Table 3, it is obvious that there is a high variability from year to year. That variability ranges from $2,145,000 to more than $10,000,000. Such a fluctuation can be a major source of uncertainty. In order to evaluate this uncertainty, a Monte Carlo simulation (Crystal Ball by Oracle) was used for the annual revenues as the simulated cells. Assuming that annual revenues follow a Uniform Distribution with a minimum value of $2,145,000 and a maximum value of $10,942,000; any value between the minimum and the maximum have an equal probability of occurrence.

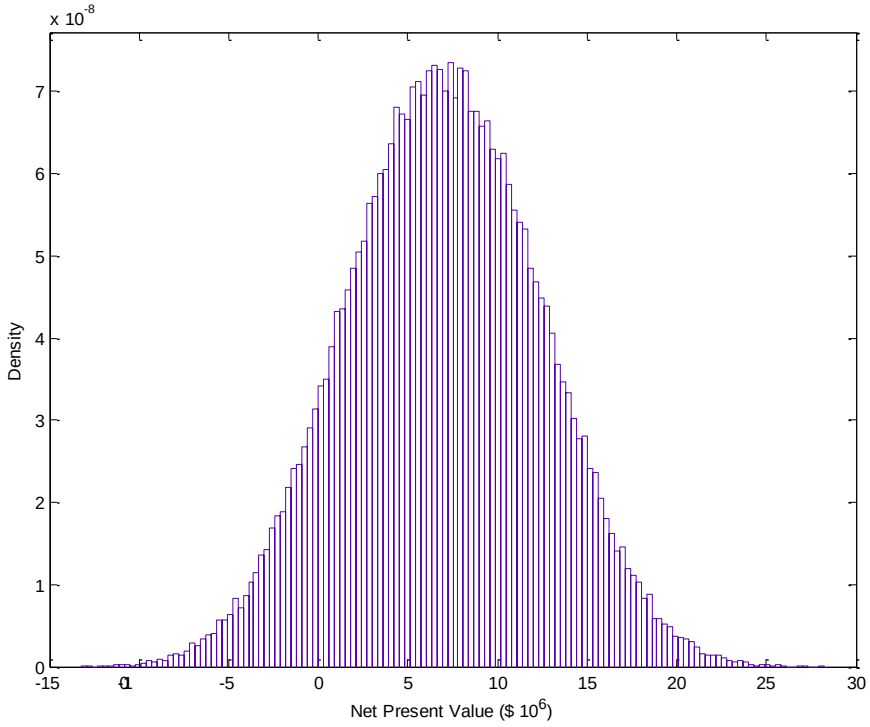

Figure 33: Evaluating the uncertainty with a Monte Carlo simulation

With a Discount rate of 10% and variable costs at 2% of revenues; a simulation was executed for 100,000 times and the resulting distribution of Net Present Value is illustrated in Figure 33. We also assume that battery is replaced every two years (in years 2, 4, 5, 8, and 10). The expected NPV is $6,975,126 and the standard deviation is $5,394,247, while the probability of negative NPV is limited to 9.9%. Hence, even after accounting for the variability in revenues there is only a small chance for this project to be without significant profits.

CHAPTER FIVE

DISCUSSION AND FUTURE WORK

In this thesis, a case study for a BESS with advanced Lead Acid batteries was developed. Two different scenarios for optimal scheduling were investigated, the first was a Photovoltaic Power Plant and the second was a Microgrid system. For both scenarios, a problem was formulated based on the attributes and constraints of each case. In both cases, the problem was solved while obtaining optimality. For the Photovoltaic Power Plant case a MILP problem formulation was developed while in the Microgrid case an LP problem formulation was developed. The optimization successfully created an ideal schedule for the BESS that maximized its usage. In essence, that means that an investment, in such a system will have a higher Return of Investment index and a faster payback time.

Furthermore, upon obtaining the revenues that the BESS generated for the Microgrid case, a financial analysis was developed. Part of the financial analysis included a brief sensitivity analysis that presented the impact of different variable costs and different discount rates. In addition, a Monte Carlo simulation was included in an attempt to address the variability, the revenues displayed throughout the lifecycle of this case study.

From this financial analysis, a few factors were neglected in an attempt to focus more on the general methodology; thus avoiding an intensive feasibility study, which is quite complicated, and goes beyond the scope of this analysis. For example, the cash flows used for this study are before taxes (income and property), therefore in reality there will be

a further reduction of the actual cash flow; which will have a negative impact on the final outcome.

On the other hand there might be incentives (e.g. subsidies) provided on a federal and a state level (USA), which were not considered, that will have a positive impact on the final outcome. Moreover, if the battery technology chosen is not Lead Acid and it is Li-Ion, then the use of refurbished batteries at a lower cost might me recommended. In [2] this approach is being evaluated as a future alternative and is based on the assumption that all the hybrid and electric cars will retire their used batteries for new ones once their capacity drops below 80 per cent. The price of these units will be significantly lower; it is projected that by 2020 the price difference might be ten times less compared to new ones. The actual value of such a system will be dictated by the supply and demand equilibrium, as shown in Figure 34. All these factors need further analysis and will be considered for future research.

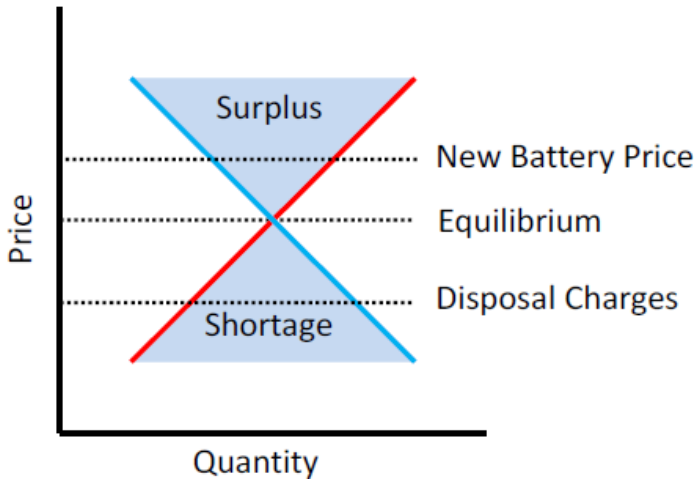

Figure 34: Factors controlling the used battery price [2]

Moreover, every battery type displays a different behavior when charged and discharged. This behavior is modeled by scientists and is a good indication of the dynamic performance of the battery. An accurate modeling is desirable, mainly for two reasons. The first reason is that the battery will display some losses and the energy used to charge the battery will be partially lost (roundtrip efficiency). The second reason is that the battery with use will degrade, therefore the nominal capacity, which the manufacturer benchmarked, will be reduced by some percentage depending usually on the number cycles and the depth of discharge. In this study battery, degradation was assumed negligible; in future, work this assumption can be addressed differently and an accurate model of the battery's behavior can be considered. That will give an extra level of accuracy to the financial analysis.

Future research might also include a comparative study of different types of battery types. The type of battery plays a significant role on a financial evaluation for many reasons. One such reason is that some batteries have a shorter lifecycle and might have to be replaced more often, thus increasing the operational costs. Other batteries, like flow batteries, with their electrolytes replenished they last up to 15 years and consequently the costs are reduced to only maintenance costs. One such example are the Vanadium Redox batteries that have a lifecycle of least 10,000 cycles which is 10 times of what a typical Lead-Acid battery will have [21]. While that sounds appealing the investor has to consider that flow batteries require a more expensive facility infrastructure.

Another reason might be, that some batteries are sensitive to operating temperatures (like Li-ion), so a more expensive facility will have to be constructed in order to

accommodate the HVAC need of those batteries. Not only the capital costs will increase but the operating costs will too, some energy will be absorbed by the BESS housing facility for its operating needs.

In conclusion the methodology developed for evaluating BESS on a Microgrid system, can serve as a tool for a financial analysis. While more accurate battery models are being created and more data about BESS costs (fixed and variable) are being shared but vendors and utilities alike this methodology can be updated and more accurate results can be obtained.

APPENDIX

State diagram for Case A

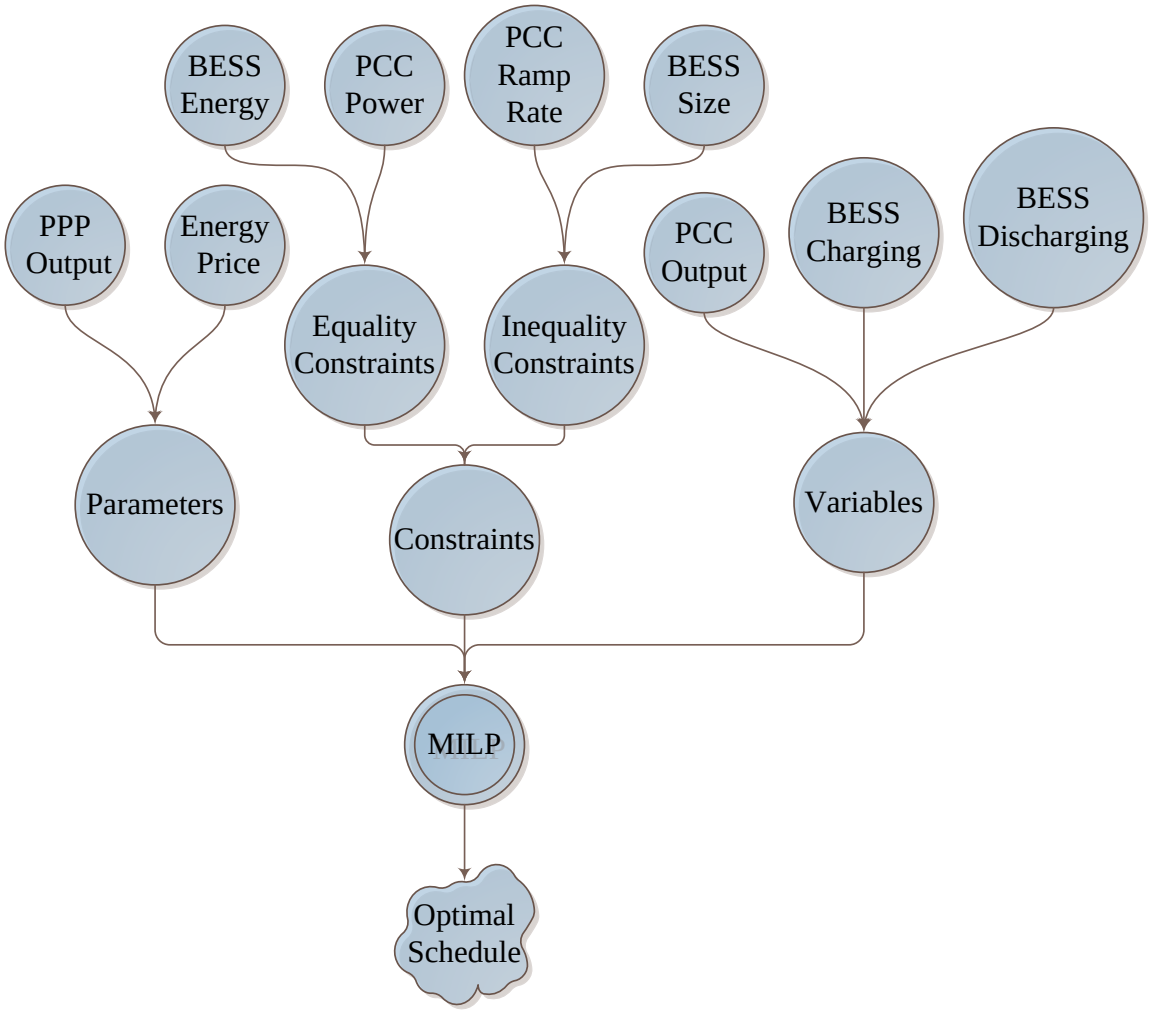

State diagram for Case B

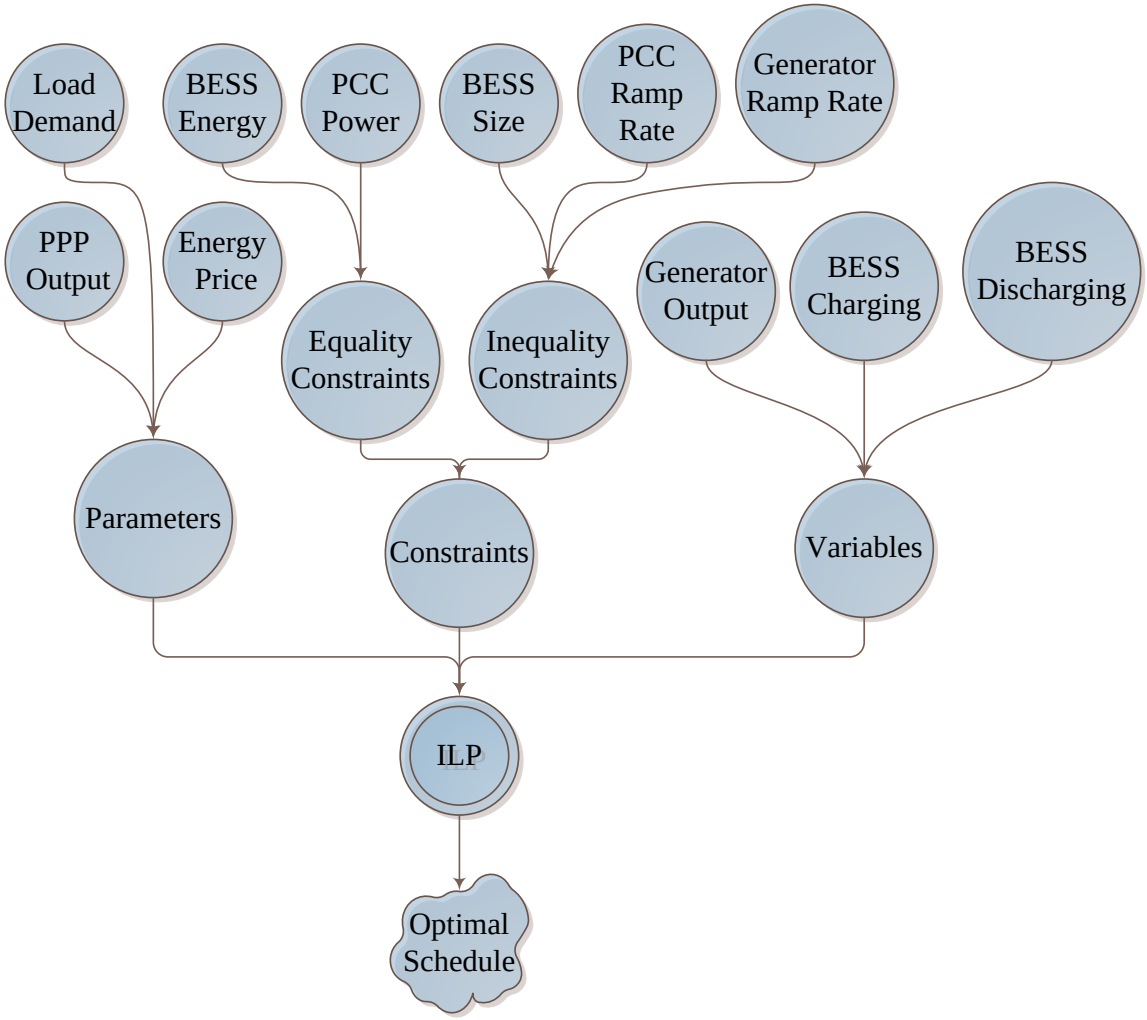

Nomenclature

P_{PV}	Active power generated by PV
P_{Bat}	Total real power at the BESS
P_{BatD}	Active power discharged from the BESS
P_{BatC}	Active power injected to the BESS
P_{BatMax}	Maximum real power stored at the BESS
P_{PCC}	Active power at the Point of Common Coupling
dP_{PCC}	Active power change at PCC at time Δt
P_{Gen}	Maximum real power generated by the generator
dP_{Gen}	Active power change at generator at time Δt
P_{Load}	Active power demand
E_{Bat}	Total energy stored at the BESS
E_{BatMax}	Maximum energy stored at the BESS
C_1	Energy price
C_2	Cost for generator operation
Δt	Incremental time between power dispatches
η_1	Efficiency when converting from DC to DC

η_2	Efficiency when converting from AC to DC
ρ_1	Generator ramp up rate
ρ_2	Generator ramp down rate
ε	Constraint for dP_{PCC}
β	BESS charge/discharge decision variable
t	Time-step

Sample of the Matlab script for Case A

```
clear all; close all; clc;

load solar_data

load cost_hoep

nDis=288; % no of dispatches 24hrs/5min = 288 dispatches / day

nVars=6; % no of variables

day_no = 1; %choose a day of the year 1-365

c = yi( day_no*(1:288),1 ); % Price of energy $/MWhr

p_pv = data(day_no,:); % PV power MWh

hours = 1; %battery duartion

p_bmax = 39; % BESS Power size

e_bmax = hours*p_bmax; % BESS Energy size

delta_up = p_bmax*1/100; % deviation from dispatch to dispatch 1%

delta_down = -p_bmax*1/100; % deviation from dispatch to dispatch 1%

p_pcc_max = 60; % PCC Power size ~1.5 of rated

n1 = 0.90; % efficiency charge DC2DC

n2 = 0.85;  % efficiency discharge DC2AC

beta1 = sparse(nDis,1); % decision making variable for charging or discharging
```

```
beta2 = sparse(nDis,1); % decision making variable for charging or discharging

dt = 5/60; % every 5min for an hour

nCons_eq=2; % no equality constraints

nCons_ineq=6; % no inequality constraints

IntVar1 = 5:nVars:nDis*nVars; % index of integer variable beta

IntVar2 = 6:nVars:nDis*nVars; % index of integer variable beta

IntVar=[IntVar1 IntVar2];

A_ineq=sparse(nCons_ineq*nDis,nVars*nDis); % size for A matrix 4 equality constraints

b_ineq=sparse(nCons_ineq*nDis,1); % size for b matrix 4 equality constraints

A_eq=sparse(nCons_eq*nDis,nVars*nDis); % size for A matrix 4 inequality constraints

b_eq=sparse(nCons_eq*nDis,1); % size for b matrix 4 inequality constraints

x_lb=sparse(nVars*nDis,1); % lower boundaries for variables

upper_limits = [p_pcc_max; p_bmax;p_bmax; e_bmax; 1; 1;];

x_ub= repmat(upper_limits,nDis,1); % upper boundaries for variables

ppcc_ind = [1 : nVars : nVars*nDis]; % index for Ppcc

for t = 1 : (nDis)

   if t == 1
```

% Equation 1: p_pcc(t) - p_bd(t) + p_bc(t) = p_pv(t) => x1 -x2 x3 Power at Point of Common Coupling

A_eq(t,[t t+1 t+2])= [1 -1 1];

b_eq(t)=p_pv(t);

% Equation 2: e_b(t) - e_b(t-1) - (p_bc(t)*dt)*n + (p_bd(t)*dt)/n = 0 => x4 0 -x3 x2 Change in power at PCC

A_eq(t+1,[t+3 t+2 t+1])= [1 -1*dt*n1 1*dt/n2];

b_eq(t+1)=0;

else

% Equation 1: p_pcc(t) - p_bd(t) + p_bc(t) = p_pv(t) => x7 -x8 x9 Power at Point of Common Coupling

A_eq((t-1)*nCons_eq+1 ,[(t-1)*nVars+1 (t-1)*nVars+2 (t-1)*nVars+3])= [1 -1 1];

b_eq((t-1)*nCons_eq+1)=p_pv(t);

% Equation 2: e_b(t) - e_b(t-1) - (p_bc(t)*dt)*n + (p_bd(t)*dt)/n = 0 => x10 -x4 -x9 x8 Change in power at PCC

A_eq((t-1)*nCons_eq+2 ,[(t-1)*nVars+4 (t-2)*nVars+4 (t-1)*nVars+3 (t-1)*nVars+2])= [1 -1 -1*dt*n1 1*dt/n2];

b_eq((t-1)*nCons_eq+2)=0;

```
    end
end
for t = 1 : (nDis-1)
    % Inequality 1: p_pcc(t) - p_pcc(t-1) <= delta          <=> x7 -x1
    A_ineq((t-1)*nCons_ineq+1,[(t-1)*nVars+7 (t-1)*nVars+1])=[1 -1];
    b_ineq((t-1)*nCons_ineq+1)=delta_up;
    % Inequality 2     delta_down<=p_pcc(t)-p_pcc(t-1)<=delta_up     <=> x7 -x1
    A_ineq((t-1)*nCons_ineq+2,[(t-1)*nVars+7 (t-1)*nVars+1])=[-1 1];
    b_ineq((t-1)*nCons_ineq+2)=-delta_down;
    % Inequality 3      p_bc(t) - p_bmax * beta1 <= 0        <=> x3 - p_bmax*x5
    A_ineq((t-1)*nCons_ineq+3,[(t-1)*nVars+3 (t-1)*nVars+5])=[1 -p_bmax];
    b_ineq((t-1)*nCons_ineq+3)=0;
    % Inequality 4      p_bd(t)- p_bmax * beta2 <= 0    <=> %x2 - p_bmax*x6
    A_ineq((t-1)*nCons_ineq+4,[(t-1)*nVars+2 (t-1)*nVars+6])=[1 -p_bmax];
    b_ineq((t-1)*nCons_ineq+4)=0;
    % Inequality 5      beta1 + beta2 <= 1    <=> %x5 + x6
    A_ineq((t-1)*nCons_ineq+5,[(t-1)*nVars+5 (t-1)*nVars+6])=[1 1];
```

```
    b_ineq((t-1)*nCons_ineq+5)=1;

    % Inequality 6      e_b <= e_bmax    <=> % x4

    A_ineq((t-1)*nCons_ineq+6,(t-1)*nVars+4)=1;

    b_ineq((t-1)*nCons_ineq+6)=e_bmax;

end

f=sparse(nVars*nDis,1); % size for f vector

f(ppcc_ind)=-c*dt; % c is of size nDis by 1

x = intlinprog(f,IntVar,A_ineq,b_ineq,A_eq,b_eq,x_lb,x_ub);

p_pcc = x([1:nVars:end,1]); %x1

p_bd = x([2:nVars:end,1]); %x2

p_bc = x([3:nVars:end,1]); %x3

e_b = x([4:nVars:end,1]); %x4

beta1 = x([5:nVars:end,1]); %x5

beta2 = x([6:nVars:end,1]); %x6

subplot(2,1,1);

plot (p_pcc,'b','LineWidth',5)

hold on
```

```
plot (p_pv,'r','LineWidth',2)

hold on

plot (-(p_bc-p_bd), 'm','LineWidth',2)

hold on

legend ('P_{PCC}','P_{PV}','P_{Battery}')

xlabel('Time dt=5min')

ylabel('Power (MW)')

title('Optimization Results for 24hrs, PV:39MW, BESS: 39MW/1hrs')

subplot(2,1,2);

plot (c,'g')

hold on

legend ('Energy Price')

xlabel('Time dt=5min')

ylabel('$/MWhr')
```

Sample of the Matlab script for Case B

```
function res=bess_lp_test(options)

close all; clc;

load solar_data; % SC PV plant 2006

load ontario_price_2014_ii; %HOEP 2006

load ontario_load_2014_ii; % Historical Hourly Ontario and Market Demands 2006

nDis=288; % no of dispatches 24hrs/5min = 288 dispatches / day

nVars=4; % no of variables

day_no = options.day_no;

e_init=0; % charge at the beginning of the day

c1 = ontario_price_2014_ii( day_no*(1:288),1 ); % Price of energy $/MWhr

p_load = ontario_load_2014_ii( day_no*(1:288),1 );

p_gen_max = max(ontario_load_2014_ii);

p_pv = data(day_no,:); % PV power MWh

hours = 1; %battery duration

p_bmax = 39; % BESS Power size

e_bmax = hours*p_bmax;% BESS Energy size
```

```
% e_bmax =e_bmax *(1-options.BESS_change); % BESS Energy size with change

ramp_up = 25; %gen ramp time 5MW/min => 25MW/5min

ramp_down = -25;

n1 = 0.90; % efficiency charge DC2DC

n2 = 0.85;  % efficiency discharge DC2AC

dt = 5/60; % every 5min for an hour

nCons_eq=2; % no equality constraints

nCons_ineq=3; % no inequality constraints

A_ineq=sparse(nCons_ineq*nDis,nVars*nDis); % size for A matrix 4 equality constraints

b_ineq=sparse(nCons_ineq*nDis,1); % size for b matrix 4 equality constraints

A_eq=sparse(nCons_eq*nDis,nVars*nDis); % size for A matrix 4 inequality constraints

b_eq=sparse(nCons_eq*nDis,1); % size for b matrix 4 inequality constraints

x_lb=zeros(nVars*nDis,1); % lower boundaries for variables

upper_limits = [p_gen_max; p_bmax;p_bmax;e_bmax]; % upper_limits:  P_gen;
P_bat_dis; P_bat_cha; E_bat; K;

x_ub= repmat(upper_limits,nDis,1); % upper boundaries for variables

for t = 1 : (nDis)

   if t == 1
```

% Equation 1: p_gen(t) + p_bd(t) - p_bc(t) = p_load - p_pv(t) => x1 x2 -x3 Power at Point of Common Coupling

A_eq(t,[t t+1 t+2]) = [1 1 -1];

b_eq(t) = p_load(t) - p_pv(t);

% Equation 2: e_b(t) - e_b(t-1) - (p_bc(t)*dt)*n + (p_bd(t)*dt)/n = 0 => x4 0 -x3 x2 Change in power at PCC

A_eq(t+1,[t+3 t+2 t+1]) = [1 -1*dt*n1 1*dt/n2];

b_eq(t+1) = 0;

else

% Equation 1: p_gen(t) + p_bd(t) - p_bc(t) = p_load - p_pv(t) => x7 x8 -x9 Power at Point of Common Coupling

A_eq((t-1)*nCons_eq+1 ,[(t-1)*nVars+1 (t-1)*nVars+2 (t-1)*nVars+3])= [1 1 -1];

b_eq((t-1)*nCons_eq+1)= p_load(t) - p_pv(t);

% Equation 2: e_b(t) - e_b(t-1) - (p_bc(t)*dt)*n + (p_bd(t)*dt)/n = 0 => x10 -x4 -x9 x8 Change in power at PCC

A_eq((t-1)*nCons_eq+2 ,[(t-1)*nVars+4 (t-2)*nVars+4 (t-1)*nVars+3 (t-1)*nVars+2])= [1 -1 -1*dt*n1 1*dt/n2];

b_eq((t-1)*nCons_eq+2) = 0;

```
    end
end
%% new constraint for Eb(tend)=Einit
A_eq(end+1,end)=1; % the last index is that of e_b(tend)
b_eq(end+1)=e_init;
for t = 1 : (nDis-1)
    % Inequality 1: p_pcc(t) - p_pcc(t-1) <= delta          <=> x7 -x1
    A_ineq((t-1)*nCons_ineq+1,[(t-1)*nVars+5 (t-1)*nVars+1])=[1 -1];
    b_ineq((t-1)*nCons_ineq+1)=ramp_up;
% % Inequality 2     delta_down<=p_pcc(t)-p_pcc(t-1)<=delta_up     <=> x7 -x1
    A_ineq((t-1)*nCons_ineq+2,[(t-1)*nVars+5 (t-1)*nVars+1])=[-1 1];
    b_ineq((t-1)*nCons_ineq+2)=-ramp_down;
    % Inequality 6      e_b <= e_bmax    <=> % x4
    A_ineq((t-1)*nCons_ineq+3,(t-1)*nVars+4)=1;
    b_ineq((t-1)*nCons_ineq+3)=e_bmax;
end
f=sparse(nVars*nDis,1); % size for f vector
```

```
p_gen_ind=1 : nVars : nVars*nDis; % index for

p_bat_dis_ind =2 : nVars : nVars*nDis; % index for

p_bat_chrg_ind =3 : nVars : nVars*nDis; % index for

%c2 = rand(length(c1),1)*30;% cost generator MWhr

c2 = ones(length(c1),1)*30;% cost generator MWhr

f(p_gen_ind) = c2*dt;

f(p_bat_chrg_ind) = c1*dt;

f(p_bat_dis_ind) = -c1*dt;

 [x,fval,exitflag,output] = linprog(f,A_ineq,b_ineq,A_eq,b_eq,x_lb,x_ub);

if exitflag~=1

 disp('ERROR: optimal solution was not obtained.')

end

 p_gen = x(1:nVars:end); %x1

 p_bd = x(2:nVars:end); %x2

 p_bc = x(3:nVars:end); %x3

 e_b = x(4:nVars:end); %x4

  if options.flg==1
```

```
plot (p_gen,'b')

hold on

stem (p_pv,'r')

hold on

plot (p_bc-p_bd, 'm')

hold on

stem (c1,'g')

hold on

plot (p_load,'k')

hold on

  legend ('P_{GEN}','P_{PV}','P_{Battery}','$/MWhr', 'load')

xlabel('Time dt=5min')

title('Optimization Results for 24hrs, 39MW/4hrs')

subplot(4,1,1);

stem (p_gen,'b')

hold on

plot (p_pv,'r','LineWidth',3)
```

```
hold on

plot (p_bd-p_bc,'m','LineWidth',3)

hold on

plot (p_load,'k','LineWidth',3)

hold on

legend ('P_{Generator}','P_{PV}','P_{Battery}','Load')

xlabel('Time dt=5min')

ylabel('Power (MW)')

title('Optimization Results for 24hrs, Generator:86MW (ramp rate:0.2MW/min), PV:39MW, BESS: 39MW/1hrs')

% title('Optimization Results for 24hrs, Generator:86MW (ramp rate:2MW/min), PV:39MW, BESS: 39MW/1hrs')

subplot(4,1,2);

stem (c1,'g')

hold on

legend ('Energy Price')

xlabel('Time dt=5min')

ylabel('$/MWhr')
```

```
subplot(4,1,3);

stem (p_bd)

hold on

stem (p_bc,'r')

legend ('discharge','charge')

xlabel('Time dt=5min')

ylabel('MW')

subplot(4,1,4);

stem (c2)

legend ('import cost')

xlabel('Time dt=5min')

ylabel('$/MWhr')

end

%% put results in results structure

res.p_gen=p_gen;

res.p_bd=p_bd;

res.p_bc=p_bc;
```

```
res.e_b=e_b;

res.profit_nDis=  ((p_load-p_pv').*c2*dt)-(-p_bd.*c1*dt-p_pv'.*c1*dt+p_gen.*c2*dt);  %
profit=cost_withoutBESS-cost_withBESS   p_load

res.profit= sum(res.profit_nDis);

res.BESS_degradation=sum(p_bc*dt)/e_bmax;

res.BESS_degradation1=sum(p_bd*dt)/e_bmax;

res.BESS_GEN_SIZE = p_gen_max;

res.output=output;

res.exitflag=exitflag;

function res=bess_lp_test(options)

clear all; close all; clc;

total_cycles=inf; %lifespan

%---- structure

options.flg=0; % 1 plots the output

options.BESS_change=0;

standard_charge=1; %SOC standard for total_cycles

profit=[];cycles_charge=[];cycles_discharge=[];

for n=1:365
```

```
        options.day_no=n;
        res=bess_lp_test(options);
        Res{n}=res; % cell output of bess_lp
    options.BESS_change=options.BESS_change+(1-
standard_charge)*(res.BESS_degradation/total_cycles); % battery degradation
    profit=[profit;res.profit];
        cycles_charge=[cycles_charge res.BESS_degradation];
        cycles_discharge=[cycles_charge res.BESS_degradation1];
end
total_profit=sum(profit)
CYCLES_charge = sum(cycles_charge)
CYCLES_dis = sum(cycles_discharge)
GEN_SIZE = res.BESS_GEN_SIZE
figure(1)
bar(profit)
xlabel('Day of year')
ylabel('Revenue from BESS ($)')
```

REFERENCES

[1] "Battery Energy Storage System," AEG Power Solutions, 2013. [Online]. Available: http://www.aegps.com/en/smart-grids/battery-energy-storage/.

[2] O.R.N.L., "Economic Analysis of Deploying Used Batteries in Power Systems.," Oak Ridge National Laboratory, Oak Ridge, Tennessee 3, 2011.

[3] "National Solar Jobs Census 2010.," The Solar Foundation, Washington, DC, 2010.

[4] G. Knier, "NASA Science," NASA, [Online]. Available: http://science.nasa.gov/science-news/science-at-nasa/2002/solarcells/. [Accessed September 2015].

[5] NREL, "SunShot Vision Study," U.S. Department of Energy, February 2012.

[6] M. Mendelsohn, T. Lowder and B. Canavan, "Concentrating Solar Power and Photovoltaics Projects: A Technology and Market Overview," U.S. National Renewable Energy Laboratory, April 2012.

[7] A. Gagliano, F. Nocera, F. Patania and A. Contino, "A procedure for the characterization of the solar-weighted reflectance of mirrored reflectors.," in *Renewable Energy Congress (IREC)*, March 2014.

[8] A. Luque and S. Hegedus, "Handbook of Photovoltaic Science and Engineering.," John Wiley & Sons, 2005.

[9] P. Mints and J. Donnelly, "Photovoltaic Manufacturer Shipments, Capacity and Competitive Analysis 2010/2011.," NREL, 2011.

[10] D. C. Jordan and S. R. Kurtz, "Photovoltaic Degradation Rates: An Analytical Review," *Progress in Photovoltaics: Research and Applications*, no. NREL/JA-5200-51664, 2012.

[11] S. Shaheen, D. Ginley and G. Jabbour, "Organic-Based Photovoltaics: Toward Low-Cost Power Generation.," *MRS Bulletin*, vol. 30, no. 1, pp. 10-15, 2005.

[12] NREL, "Best Research-Cell Efficiencies.," National Renewable Energy Laboratory, 2011. [Online]. Available: http://www.nrel.gov/ncpv/images/efficiency_chart.jpg. [Accessed September 2015].

[13] H. Schütt, "PV Magazine: A market in movement.," Solarpraxis AG, March 2010. [Online]. Available: http://www.pv-magazine.com/typo3temp/pics/03055-maintypesoftrackerspdf_6a672d1c83.jpg. [Accessed September 2015].

[14] K. Mertens, Photovoltaics : Fundamentals, Technology and Practice., Somerset, NJ: John Wiley & Sons, 2013.

[15] "Green Energy Innovations," [Online]. Available: http://www.geinnovations.net/solar_net_metering.html. [Accessed November 2015].

[16] A. Ter-Gazarian, Energy Storage for Power Systems., London, United Kingdom: The Institution of Engineering and Technology, 2011.

[17] "Consumers Energy," [Online]. Available: https://www.consumersenergy.com/uploadedfiles/ceweb/shared/ludingtonpumpedstorage.pdf. [Accessed October 2015].

[18] E. Barbour, "Energy Storage Sense," [Online]. Available: http://energystoragesense.com/compressed-air-energy-storage/. [Accessed October 2015].

[19] Sandia-NL, "DOE/EPRI 2013 Electricity Storage Handbook in Collaboration with NRECA," U.S. Department of Commerce, Albuquerque, New Mexico, 2013.

[20] D.O.E., "Grid Energy Storage," U.S. Department of Energy, 2013.

[21] R. Baxter, Energy Storage: A Nontechnical Guide, Tulsa, Oklahoma: PennWell Corporation, 2006.

[22] EPRI, "Energy Storage System Costs 2011 Update - Executive Summary," May 2015. [Online]. Available: http://www.eosenergystorage.com/documents/EPRI-Energy-Storage-Webcast-to-Suppliers.pdf. [Accessed May 2015].

[23] K. Cordtz and P. Genzer, "Grant Funds Superconducting Magnet Energy Storage Research at Brookhaven Lab.," August 2010. [Online]. Available: https://www.bnl.gov/newsroom/news.php?a=11174. [Accessed October 2015].

[24] Y. Wang, "Concentrated Solar Power," 2008. [Online]. Available: https://www.mtholyoke.edu/~wang30y/csp/PTPP.html. [Accessed November 2015].

[25] G. G. Botte and M. Muthuvel, "Electrochemical Energy Storage: Applications, Processes, and Trends," in *Handbook of Industrial Chemistry and Biotechnology*, Springer, 2012, pp. 1497-1539.

[26] D. Darlin, "The Worlds of David Darling," [Online]. Available: http://www.daviddarling.info/encyclopedia/N/AE_NAS_battery.html. [Accessed November 2015].

[27] "UC Davis ChemWi," [Online]. Available: http://chemwiki.ucdavis.edu/Analytical_Chemistry/Electrochemistry/Case_Studies/Commercial_Galvanic_Cells. [Accessed November 2015].

[28] S. Ye, "Mobile Nations," 2 January 2015. [Online]. Available: http://www.androidcentral.com/smartphone-futurology-1-battery. [Accessed November 2015].

[29] SBC, "Electricity Storage: Leading the Energy Transition," SBC Energy Institute, 2013.

[30] EPRI, "Electricity Energy Storage Technology Options: A White Paper Primer on Applications, Costs, and Benefits," ELECTRIC POWER RESEARCH INSTITUTE, Palo Alto, California, 2010.

[31] H. Chen, T. Cong, W. Yang and C. Tan, "Progress in Electrical Energy Storage System: A Critical Review," *Progress in Natural Science,* 2009.

[32] H. Qian, J. Zhang, J.-S. Lai and W. Yu, "A high-efficiency grid-tie battery energy storage system.," *IEEE Transactions on Power Electronics,* vol. 26, no. 3, pp. 886-896, 2011.

[33] C. Hill, M. Such, D. Chen, J. Gonzalez and W. Grady, "Battery Energy Storage for Enabling Integration of Distributed Solar Power Generation," *IEEE Transactions on Smart Grid,* vol. 3, no. 2, pp. 850-857, 2012.

[34] B. Kroposki and G. Martin, "Hybrid renewable energy and microgrid research work at NREL.," in *IEEE Power and Energy Society General Meeting,* 2010.

[35] J. W. Shim, Y. Cho, S.-J. Kim, S. W. Min and K. Hur, "Synergistic Control of SMES and Battery Energy Storage for Enabling Dispatchability of Renewable Energy Sources.," *IEEE Transactions Applied Superconductivity.,* vol. 23, no. 3, p. 57012.

[36] C. Hill, M. Such, D. Chen, J. Gonzalez and W. Grady, " "Battery Energy Storage for Enabling Integration of Distributed Solar Power Generation,"," *IEEE Transactions on Smart Grid,* vol. 3, no. 2, pp. 850-857, 2012.

[37] M. Lawder, B. Suthar, P. Northrop, S. De, C. Hoff, O. Leitermann, M. Crow, S. Santhanagopalan and V. Subramanian, "Battery Energy Storage System (BESS) and

Battery Management System (BMS) for Grid-Scale Applications.," *Proceedings of the IEEE,* vol. 102, no. 6, pp. 1014-1030, 2014.

[38] P.I.E.R., "2020 Strategic Analysis Of Energy Storage In California.," California Energy Commission, 2011.

[39] B. McKeon, J. Furukawa and S. Fenstermacher, "Advanced Lead–Acid Batteries and the Development of Grid-Scale Energy Storage Systems.," *Proceedings of the IEEE,* vol. 102, no. 6, pp. 951-963, 2014.

[40] EPRI, "Electricity Energy Storage Technology Options: A White Paper Primer on Applications, Costs, and Benefits.," EPRI, Palo Alto, CA, 2010.

[41] S. N. Laboratories, "Energy Storage for the Electricity Grid: Benefits and Market Potential Assessment Guide," U.S. Department of Commerce, Springfield, VA, 2010.

[42] J. Waight, F. Albuyeh and A. Bose, "Scheduling of Generation and Reserve Margin Using Dynamic and Linear Programming.," *IEEE Transactions on Power Apparatus and Systems,* Vols. PAS-100, no. 5, pp. 2226-2230, 1981.

[43] G. Chang, M. Aganagic, J. Waight, J. Medina, T. Burton, S. Reeves and M. Christoforidis, "Experiences with mixed integer linear programming based approaches on short-term hydro scheduling.," *IEEE Transactions on Power Systems,* vol. 16, no. 4, p. 74.

[44] "Solar Power Data for Integration Studies.," NREL, 2006. [Online]. Available: http://www.nrel.gov/electricity/transmission/. [Accessed May 2015].

[45] "Ontario Electricity Prices & the Wholesale Market," Independent Electricity System Operator (IESO), 2015. [Online]. Available: http://www.ieso.ca/. [Accessed May 2015].

[46] "DOE/EPRI 2013 Electricity Storage Handbook in Collaboration with NRECA.," Sandia National Laboratories, Albuquerque, New Mexico, 2013.

[47] S. M. Schoenung and J. Eyer, "Benefit/Cost Framework for Evaluating Modular Energy Storage: A Study for the DOE Energy Storage Systems Program," Sandia National Laboratories, Albuquerque, New Mexico, 2008.